

Review

Open Access



Single-atom catalysts for (photo)electrocatalytic biomass valorization to high-value-added chemicals

Jing Ma¹, Hao Yan¹, Xu Hou², Ming Xu¹, Tingting Cui¹

¹College of Chemistry, Chemical Engineering & Resource Utilization, Center for Innovative Research in Synthetic Chemistry and Resource Utilization, Northeast Forestry University, Harbin 150040, Heilongjiang, China.

²School of Chemical Engineering, Changchun University of Technology, Changchun 130012, Jilin, China.

Correspondence to: Prof. Tingting Cui, College of Chemistry, Chemical Engineering & Resource Utilization, Center for Innovative Research in Synthetic Chemistry and Resource Utilization, Northeast Forestry University, No. 26 Hexing Road, Xiangfang District, Harbin 150040, Heilongjiang, China. E-mail: ttcui@nefu.edu.cn; Prof. Ming Xu, College of Chemistry, Chemical Engineering & Resource Utilization, Center for Innovative Research in Synthetic Chemistry and Resource Utilization, Northeast Forestry University, No. 26 Hexing Road, Xiangfang District, Harbin 150040, Heilongjiang, China. E-mail: mingxu@nefu.edu.cn; Prof. Xu Hou, School of Chemical Engineering, Changchun University of Technology, No. 2055 Yan'an Street, Changchun 130012, Jilin, China. E-mail: houx@ccut.edu.cn

How to cite this article: Ma, J.; Yan, H.; Hou, X.; Xu, M.; Cui, T. Single-atom catalysts for (photo)electrocatalytic biomass valorization to high-value-added chemicals. *Microstructures* 2025, 5, 2025002. <https://dx.doi.org/10.20517/microstructures.2024.38>

Received: 30 Apr 2024 **First Decision:** 4 Jun 2024 **Revised:** 14 Jun 2024 **Accepted:** 25 Jun 2024 **Published:** 14 Jan 2025

Academic Editors: Liangzhi Kou, Sarina Sarina, Dingsheng Wang **Copy Editor:** Fangyuan Liu **Production Editor:** Fangyuan Liu

Abstract

As a crucial renewable energy resource, biomass can be converted into high-value-added chemicals via unique catalytic routes, which facilitate the reduction of excessive dependency on fossil resources. However, the complex functional groups inherent in biomass and biomass-derived compounds enable considerable difficulties for their selective functionalization. The precise cleavage of special chemical bonds in biomass highly depended on the structure design of catalysts. Single-atom catalysts (SACs) have garnered significant attention in biomass valorization through the electrocatalytic and photoelectrocatalytic processes due to their maximal atom utilization efficiency, unique electronic structure, and tunable coordination environments. The present review outlines the latest research progress in this emerging field, focusing on the (photo)electrocatalytic application of SACs in biomass valorization, including cellulose-derived and hemicellulose-derived compounds and lignin. We also emphasize the innovative design and precise modulation of atomically dispersed metal active sites at the atomic level. Through state-of-the-art catalytic systems, we elaborately discuss the structure-activity relationship and elucidate the mechanisms of the (photo)electrocatalytic processes over SACs. Finally, we provide the prospects of SACs in (photo)electrocatalytic biomass valorization.

Keywords: Single-atom catalysts, biomass valorization, electrocatalysis, photoelectrocatalysis



© The Author(s) 2025. **Open Access** This article is licensed under a Creative Commons Attribution 4.0 International License (<https://creativecommons.org/licenses/by/4.0/>), which permits unrestricted use, sharing, adaptation, distribution and reproduction in any medium or format, for any purpose, even commercially, as long as you give appropriate credit to the original author(s) and the source, provide a link to the Creative Commons license, and indicate if changes were made.



INTRODUCTION

Biomass, as the only form of renewable carbon resource, has great advantages for preparing fine chemicals replacing fossil resources, such as abundant supply, widespread distribution, zero CO₂ emissions, and recycling utilization. It is the fourth-largest energy source, following only oil, coal, and natural gas. With the increasingly serious shortage of fossil energy and environmental pollution, the high-value utilization of biomass-based platform molecules as a renewable and clean resource has become an important worldwide research topic^[1]. Among biomass existence forms, lignocellulosic biomass is the most abundant, with readily available sources and a fast regeneration rate, making it a promising alternative to petroleum resources^[2]. Lignocellulosic biomass is composed of cellulose (40%-60%), hemicellulose (20%-40%) and lignin (an aromatic oxygen-containing polymer, 10%-25%)^[3,4]. After hydrolysis of cellulose and hemicellulose, hexose (mannose, glucose, galactose)^[5] and pentose (xylose, arabinose) can be obtained, which can be further dehydrated to obtain 5-hydroxymethylfurfural (HMF)^[6,7], furfural (FUR)^[8], 2-methylfuran (2-MF), glycerol, ethanol^[9], methanol^[10] and other biomass platform compounds. Lignin mainly comprises three phenylpropane structures (syringyl, guaiacyl, and hydroxyphenyl)^[11]. By breaking the C-C bond, it is converted into highly functional monomer aromatic compounds^[12-14]. These compounds can be used as fine chemicals directly, and they can also continue to be converted directly or indirectly into a variety of valuable compounds through reduction or oxidation routes.

In the early years, the study on the valorization of biomass-based platform molecules is mainly based on thermal catalytic upgrading^[4,15,16]. It includes homogeneous catalytic systems (organic metal complexes, metal salts, *etc.*)^[17-19] and heterogeneous catalytic systems (bulk metal oxides, supported noble metals, *etc.*)^[20]. However, homogeneous catalysts present certain drawbacks, including challenges in product separation, catalyst recoverability, thermal stability, and the treatment of harmful by-products. The reported thermal catalytic systems often require high temperature and pressure conditions with longer reaction times for better product yields. Therefore, it is urgent to develop new methods for biomass valorization under mild conditions.

Due to the dual impact of energy shortage and environmental crisis, the development of catalytic conversion processes driven by renewable energy (wind, solar, tidal energy, *etc.*) has attracted wide attention^[21-32]. Advanced catalytic technologies, such as photoelectrocatalysis and electrocatalysis, offer significant advantages in catalysis. Firstly, photoelectrocatalysis and electrocatalysis can stimulate the electronic structure of reactant molecules through external energy (light or electric energy) and reduce the activation energy of the reaction, thus enabling highly efficient catalytic transformations under conditions that are beyond the reach of traditional thermal catalytic reactions. Secondly, these two catalytic methods can precisely control catalytic reactions. By adjusting the external light intensity or current density, the reaction rate, selectivity, and product distribution can be precisely controlled. Furthermore, photoelectrocatalysis and electrocatalysis can usually be carried out under milder conditions, reducing energy consumption and environmental pollution, which aligns with the development trend of green catalysis. In contrast to traditional thermal catalysis, these two approaches have a more extensive range of applications and can catalyze reactions that are challenging to achieve through conventional thermal catalysis, such as photocatalytic water decomposition and electrochemical synthesis. (Photo)electrocatalytic processes offer prospects for synthesizing value-added chemicals using biomass-based platform molecules under mild reaction conditions, which are easy to control and environmentally friendly. These methods are expected to become highly efficient green technologies for energy sustainable development^[33,34]. Intermediates or free radicals generated from biomass dehydrogenation can further transform into multicarbon compounds through carbon-carbon coupling reactions^[35,36]. However, achieving effective C-H

activation and controllable C-C coupling in photoelectrochemical/electrocatalytic biomass valorization remains challenging. The kinetic barrier of C-C coupling on metal sites of single- or dual-atom catalysts and the modulation of intermediate adsorption strength are critical factors influencing catalytic performance^[36,37]. Yang *et al.* elucidated the reasons behind the continued difficulty in carbon-carbon coupling on dual-atom electrocatalysts, providing new insights for enhancing reaction selectivity and activity^[37]. A primary hurdle in (photo)electrocatalytic biomass conversion lies in crafting cutting-edge catalysts that exhibit selectivity, stability, and superior performance in operando conditions.

Single-atom catalysts (SACs) are a unique type of supported metal catalysts with almost 100% of the metal atoms exposed on the surface, providing outstanding catalytic efficiency, activity, and selectivity. These catalysts offer distinctive advantages over metals and metal X-ides. They feature individual metal atoms as active sites, which enables precise catalytic activity and influences reaction selectivity in a manner that differs from that of metal or oxide particles, reducing catalyst usage. Furthermore, the atomic-level dispersion of SACs confers increased resistance to poisoning, thereby enhancing stability and prolonging the lifespan of the catalyst. The effective adsorption and deactivation of toxic substances achieve this. Moreover, the tunability of SACs at the atomic level allows for the optimization of catalytic performance by adjusting the metal type, number, and positioning, thereby enabling the customization of the catalyst for diverse reaction requirements.

The stability of metal atoms within the SAC structure is a significant challenge. The interaction between metal atoms and the support in SACs significantly influences the dispersion and stability of these metal atoms. Enhanced metal-support interactions can stabilize the position of metal atoms and consequently elevate the stability of the catalyst. This can be achieved through engineered designs at the atomic scale or by introducing specific ligands to stabilize metal atoms. The stability of SACs under varying environmental conditions is also a crucial consideration. For instance, elevated temperatures, pressures, or oxidative/reductive environments may trigger catalyst deactivation or degradation. Additionally, the stability of SACs during repeated usage or recycling processes is paramount. The catalyst should uphold stable catalytic activity and selectivity throughout these cycles. Recently, a spectrum of synthesis methods for SACs has been reported, with precise control over synthesis conditions to enhance catalyst stability.

SACs have garnered significant research attention over the past decade due to their great potential to significantly enhance catalytic activity and selectivity with high catalyst atomic economy^[38-46]. They have exhibited excellent catalytic performance in numerous thermocatalytic reactions involving biomass-based platform molecules^[47-56]. Several reviews on their application in biomass valorization have been reported^[43,57,58]. Vasconcelos *et al.* provided a comprehensive overview of the utilization of SACs and single-atom alloys (SAA) for enhancing the catalytic conversion of carbohydrates, formic acid, and other molecules. They also focused on the preparation and characterization of these materials and gain an insight into the potential mechanisms involved during the reactions^[43]. De *et al.* summarized recent studies on SAC applications in selectively transforming biomass-based platform molecules into value-added products, highlighting their unique catalytic activities and discussing fundamental insights into their superior performance^[57]. Wang *et al.* presented a comprehensive review of defect engineering in preparing SACs and provided an in-depth analysis of upgrading biomass-based platform molecules using SACs^[59]. Lu *et al.* reviewed examples of fuels and value-added chemicals production from biomass-based platform molecules and CO₂ using SACs^[60].

SACs play a central role in electrocatalytic and photoelectrocatalytic reactions, although significant differences exist in their structures, properties, applications, and mechanisms of action. In electrocatalysis,

SAC-based electrocatalysts are typically composed of carbon supports or metal oxides as substrate materials, with single atoms dispersed on the surface by *in situ* reduction or physical adsorption techniques. These catalysts modulate the electronic structure of surface adsorption states and active sites, facilitating electron transfer and controlling reaction pathways to achieve efficient electrocatalytic conversions. Conversely, photoelectrocatalysts for light-driven catalysis typically require manipulating material band structures and surface morphologies to enable efficient light absorption and separation of photogenerated carriers, thereby enhancing photocatalytic performance. As a result, SACs for photoelectrocatalysis must possess excellent electrocatalytic capabilities and demonstrate proficient light absorption and photogenerated carrier separation capabilities to utilize light energy fully for catalytic activation.

In recent years, significant research efforts have been devoted to biomass valorization using SACs through electrocatalytic and photoelectrocatalytic methods, aiming to convert efficiently biomass-based compounds into valuable chemicals and fuels^[61]. However, detailed reviews have not been reported on the (photo)electrocatalytic conversion of biomass-based compounds using SACs. This review summarizes recent state-of-the-art research on biomass valorization via the (photo)electrocatalytic approaches, highlighting the remarkable performance of SACs in biomass catalytic upgrading. Specifically, we focus on the (photo)electrocatalytic application of SACs for biomass-based compounds, providing illustrative examples. Additionally, the unique structure-activity relationship is discussed in detail. We also elucidate the mechanisms of the (photo)electrocatalytic processes facilitated by SACs. Finally, we provide the prospects of SACs in electrocatalytic biomass conversion.

SACS FOR CELLULOSE AND HEMICELLULOSE DERIVED MOLECULES VALORIZATION

Biomass valorization can be achieved both at the anode and the cathode. The anodic electrocatalytic oxidation (ECO) reaction is pivotal in this area and has been thoroughly researched. The high-value-added oxidative products (2,5-furandicarboxylic acid (FDCA), gluconic acid, formate, *etc.*) are key intermediates in the pharmaceutical and chemical industry.

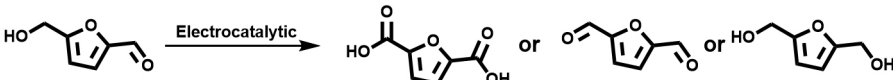
The upgrading of aldehyde compounds

After the hydrolysis of cellulose and hemicellulose, sugar compounds are produced, which subsequently undergo dehydration, retro-aldol condensation, or other reactions to generate aldehyde compounds such as HMF and FUR. These products hold significant promise in biomass conversion and utilization, which can be utilized to prepare biomass-based chemicals, such as biofuels and other high-value-added compounds.

Electrocatalytic upgrading of HMF

The electrooxidation process can convert HMF into high-value-added products [Table 1]. Among the oxidation products of HMF, FDCA emerges as exceptionally promising. Not only can it substitute terephthalic acid, a petroleum-derived monomer used in various polyesters, in the synthesis of biodegradable polymers, but it is also widely utilized as an important intermediate for fragrances and as a chelating agent of metals, among other uses. SACs have been extensively designed for the HMF oxidation reaction (HMFOR). Metal oxide supports-confined noble metal single atoms represent one type of SAC. Due to the electron interaction between the metal single atoms and oxide support, the electron density at various atomic sites will be redistributed. This can regulate the adsorption energy of HMF and intermediates, thus enhancing the electrocatalytic performance of HMFOR.

In 2021, Lu *et al.* reported an Ir-Co₃O₄ catalyst for HMFOR^[62]. High-angle annular dark-field scanning transmission electron microscopy (HAADF-STEM) characterization showed that the SAC was composed of highly dispersed Ir. The linear sweep voltammetry (LSV) curves show a lower onset potential and higher

Table 1. Various SACs for HMF valorization


Entry	Catalyst	Catalytic activity	Ref.
1	Ir-Co ₃ O ₄	98% FE, 98% FDCA yield	[62]
2	Ru ₁ -NiO	42.5% DFF yield	[63]
3	Ru/CoO _x	55.2% FE, 76.5% FDCA selectivity, and 55.0% FDCA yield	[64]
4	Ru _{0.3} /NiFe LDH	99.24% FDCA selectivity and 98.68% FDCA yield	[65]
5	Rh-SA/NiFe NMLDH	Nearly 100% FE, long-term stability of more than 100 h	[66]
6	Ru ₁ Cu SAA	0.47 mmol cm ⁻² h ⁻¹ DHMF formation rate, 85.6% FE	[67]

current density for Ir-Co₃O₄ than Co₃O₄ and IrO₂. This indicates that HMFOR has higher activity on Ir-Co₃O₄ than that on Co₃O₄, which may be due to Ir atoms. The open-circuit potential (OCP) exhibits a more pronounced decrement with the Ir-Co₃O₄ electrode compared to the Co₃O₄ electrode, suggesting enhanced surface adsorption of HMF on Ir-Co₃O₄ [Figure 1A]. In comparison, the adsorption behavior of the catalyst for different groups demonstrates that the presence of Ir atoms can enhance its electrocatalytic performance, especially with substrates containing conjugated cyclic carbons. The temperature-programmed desorption (TPD) measurements and density functional theory (DFT) calculation imply that the enhanced adsorption of HMF on Ir-Co₃O₄ should be attributed to the C=C group rather than the C=O group [Figure 1B-E]. The Ir-Co₃O₄ SAC provided a full HMF conversion, high faradaic efficiency (FE) (98%) and FDCA yield (98%) at 1.42 V *vs.* Reversible Hydrogen Electrode (RHE, Table 1, entry 1), whereas the Co₃O₄ catalyst yielded only 90% FDCA, suggesting that the single-atom Ir can tune the adsorption energy of the HMF and contribute faster reaction kinetics [Figure 1F].

Ge *et al.* achieved efficient selective oxidation of biomass-derived alcohols, resulting in various high-value-added aldehyde products, using a single-atom ruthenium catalyst supported on oxidized nickel (Ru₁-NiO) that they developed in 2022^[63]. Experimental analysis indicates that neutral electrolytes are more favorable for the generation of aldehyde products, such as 2,5-diformylfuran (DFF), compared to common alkaline electrolytes. X-ray photoelectron spectroscopy (XPS) and X-ray absorption near-edge structure (XANES) measurements revealed that the oxidation state of Ru in Ru₁-NiO is between +3 and +4 [Figure 2A and B]. In the neutral electrolyte, Ru₁-NiO exhibits high activity for the oxidation of HMF; under low HMF conversion (< 2%), the maximum yield of DFF can reach 42.5% [Figure 2C], with 90% DFF selectivity at 1.5 V *vs.* RHE (Table 1, entry 2). Cyclic voltammetry (CV) analysis showed that the potential corresponding to the oxidation peak decreased from 1.36 to 1.14 V *vs.* RHE after loading single-atom Ru, which proved that Ru single atom significantly promoted the hydrolysis separation [Figure 2D and E]. Raman spectrometric analysis showed that the NiO carrier did not undergo reconfiguration during the catalytic process, so the reaction mechanism was consistent with the catalytic process involving OH* reported in the literature, rather than the indirect oxidation mechanism mediated by NiOOH [Figure 2F]. Ru single atoms effectively facilitate water dissociation, leading to the generation of OH* species that significantly enhance the performance of HMFOR. In contrast, in alkaline electrolytes, the formyl groups of HMF are rapidly oxidized, preventing the accumulation of aldehyde products.

In 2023, Gu *et al.* reported a single-atom Ru catalyst with a 0.5 wt% Ru loading anchored on the surface of CoO_x, wherein the presence of Ru played a crucial part in enhancing HMFOR activity^[64]. HAADF-STEM shows that the Ru species are atomically dispersed on the CoO_x substrate [Figure 3A]. The X-ray diffraction (XRD) pattern reveals the absence of distinct diffraction peaks corresponding to Ru or RuO₂, indicating a

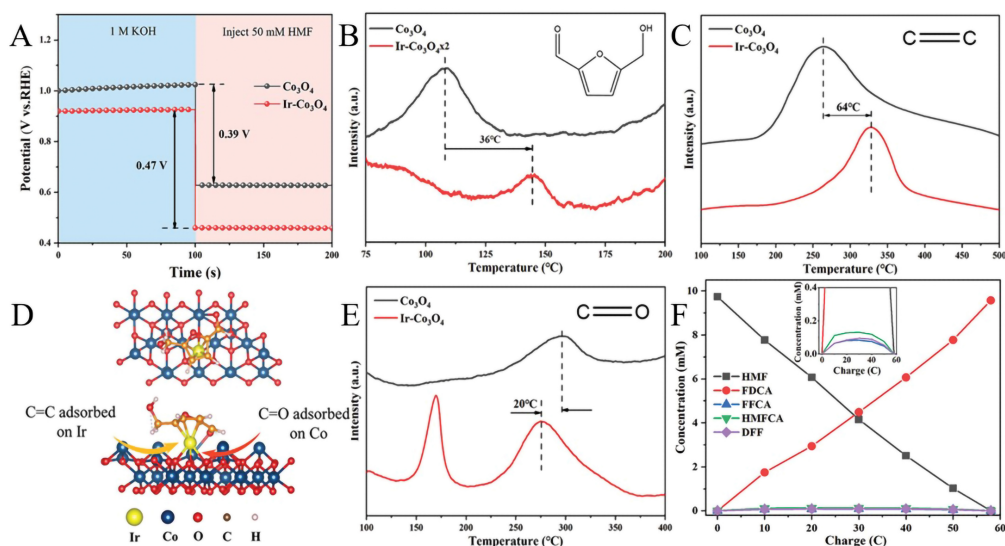


Figure 1. (A) OCP curves of Ir-Co₃O₄ and Co₃O₄. TPD spectra of Ir-Co₃O₄ and Co₃O₄ at HMF/He (B), ethylene (C), and CO (E) atmospheres. (D) The adsorption model of HMF molecules on Ir-Co₃O₄. (F) The electrocatalytic performance of Ir-Co₃O₄. Copyright 2021, Wiley^[62].

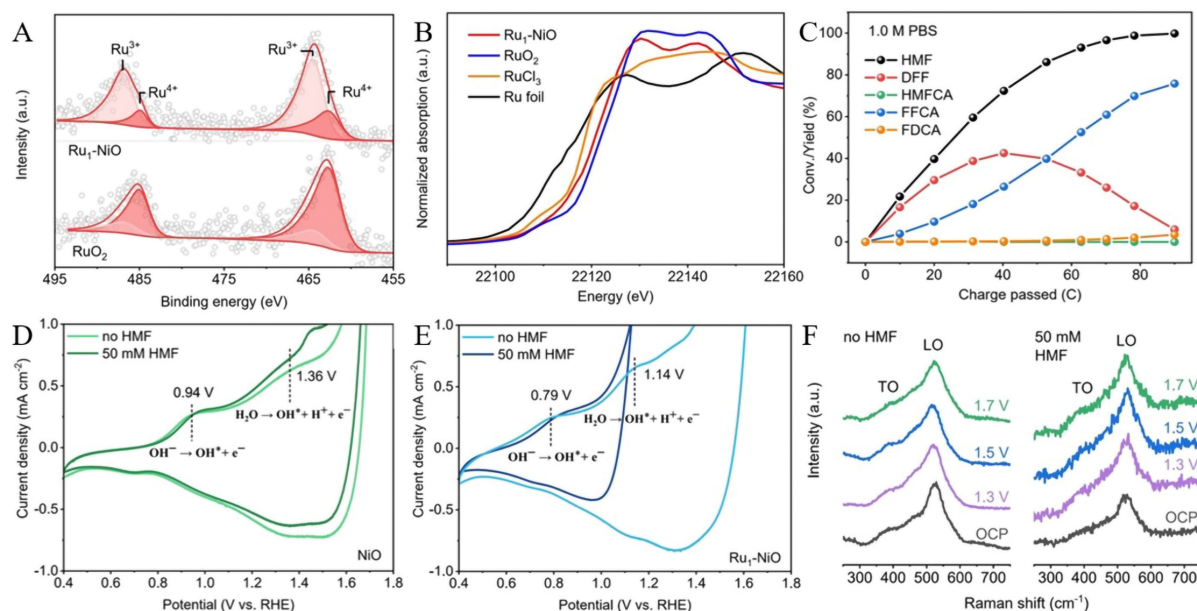


Figure 2. (A) XPS spectra of Ru 3p for Ru₁-NiO. (B) XANES spectra of Ru K-edge. (C) The electrocatalytic performance of Ru₁-NiO. CV curves of (D) NiO, (E) Ru₁-NiO. (F) The *ex situ* Raman spectra of Ru₁-NiO. Copyright 2022, Wiley^[63].

high degree of dispersion for Ru on ultrathin CoO_x [Figure 3B]. XPS and CV results have shown that the single atom Ru can increase the proportion of Co³⁺ in CoO_x and accelerate the reaction kinetics for generating active species of Co⁴⁺ [Figure 3C and D]. Notably, as shown in Figure 3E, Ru/CoO_x exhibited significantly superior HMFOR performance compared to CoO_x catalysts. Furthermore, a more significant reduction of OCP (0.4 V) was observed for the single-atom Ru/CoO_x electrode compared to that of the contrasting catalyst electrodes, demonstrating stronger surface adsorption of HMF on single-atom Ru/CoO_x [Figure 3F]. From the HMF electrolysis, a FE of 55.2%, FDCA selectivity of 76.5%, and a yield of 55.0% were

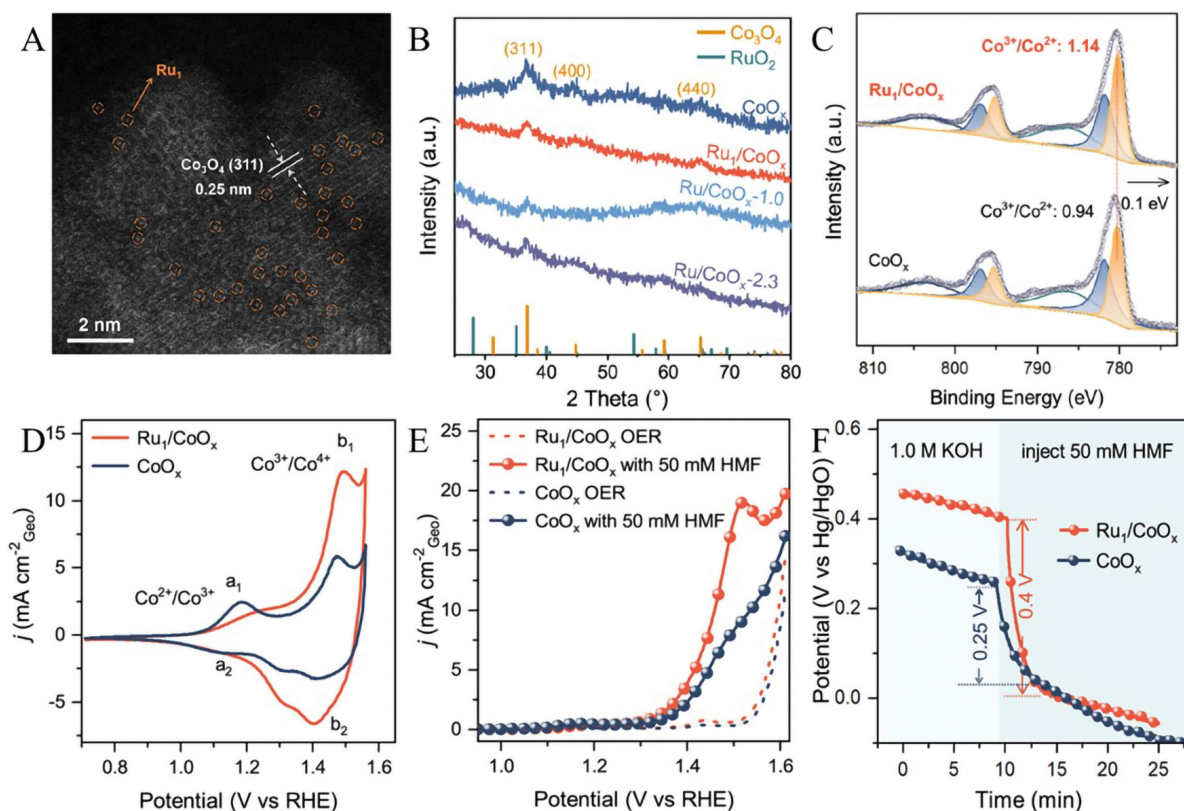


Figure 3. (A) AC HAADF-STEM image of Ru_1/CoO_x . (B) XRD pattern and (C) XPS spectra of Co 2p for CoO_x and Ru_1/CoO_x . (D) CV curves of Ru_1/CoO_x and CoO_x . (E) LSV curves of Ru_1/CoO_x and CoO_x . (F) OCP curves of Ru_1/CoO_x and CoO_x . Copyright 2023, ACS^[64].

obtained (Table 1, entry 3). This takes place via the HMFCFA pathway, as evidenced by high-performance liquid chromatography (HPLC). The single-atom Ru/CoO_x electrode exhibited excellent cyclic stability for HMFOR.

NiFe layered double hydroxide (LDH) catalyst has widely been studied for HMFOR and oxygen evolution reaction (OER). In order to enhance the number of active sites, extensive research has been conducted on the incorporation of single atoms onto the surface of NiFe-LDH, thereby maximizing atom utilization efficiency. Regarding noble metals, the exceptional cost-effectiveness of Ru, combined with the optimal bond strength between Ru and the intermediate species, distinguishes the single-atom Ru catalyst in terms of its outstanding performance.

Xu *et al.* reported a $\text{Ru}_{0.3}/\text{NiFe}$ LDH catalyst for HMFOR, which was synthesized using the two-step electrodeposition technique [Figure 4A]^[65]. Raman spectroscopic characterization confirmed the presence of high valence NiOOH as the reactive species. Doping of Ru into the crystal structure of NiFe-LDH modifies its electronic structure, thereby enhancing the adsorption energy of HMF and intermediate species [Figure 4B]. Single Ru atom also facilitated the conversion of HMF to DFF. $\text{Ru}_{0.3}/\text{NiFe}$ LDH demonstrated remarkable performance with an HMF conversion efficiency of 99.43%, an FDCA selectivity of 99.24%, and a yield of 98.68% (Table 1, entry 4).

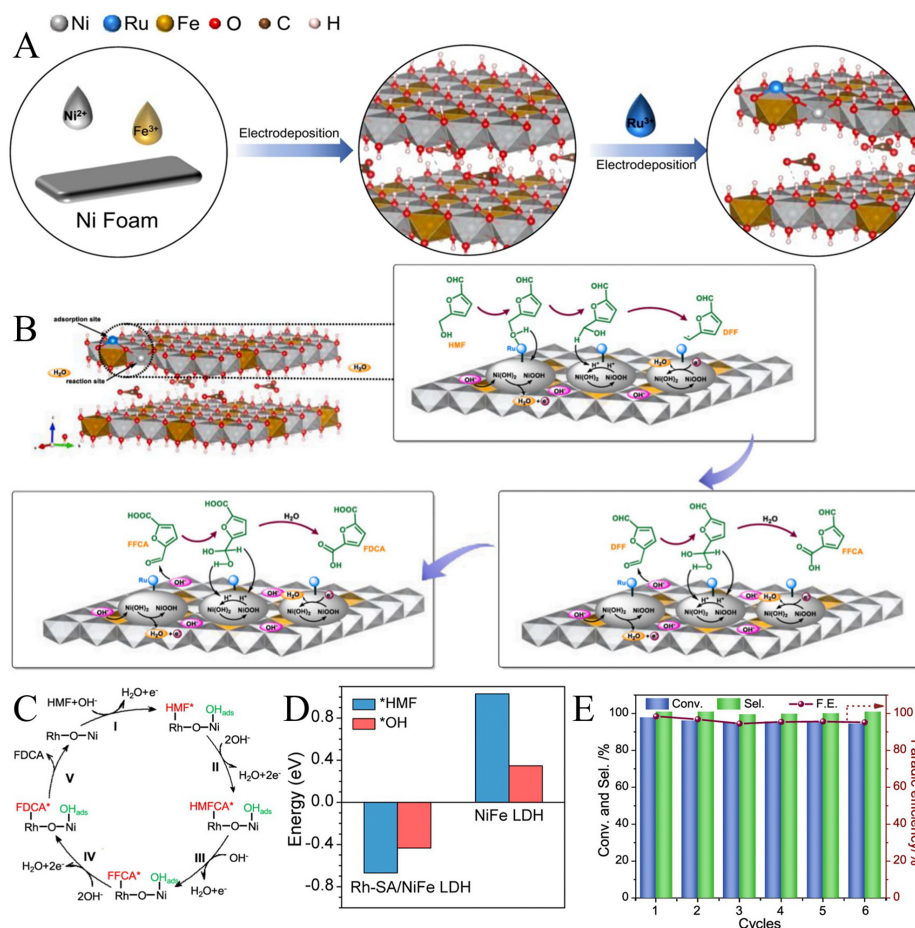


Figure 4. (A) The synthesis strategy for $\text{Ru}_{0.3}/\text{NiFe}$ LDH catalyst. (B) $\text{Ru}_{0.3}/\text{NiFe}$ catalytic process of HMFOR. Copyright 2023, Elsevier^[65]. (C) Schematic illustration of the HMFOR mechanism over Rh-SA/NiFe NMLDH. (D) The adsorption energy comparisons of HMF and $^*\text{OH}$. (E) The electrochemical cycling stability of Rh-SA/NiFe LDH. Copyright 2023, ACS^[66].

In 2023, Zeng *et al.* reported the design and preparation for a catalyst with a 1.27 wt% Rh loading, anchored on the surface of nanoporous mesh-type NiFe LDH (Rh-SA/NiFe NMLDH)^[66]. Based on the mechanistic studies, they proposed that the presence of Rh at the atomic level not only facilitates the promotion of chemisorption and activation of HMF, but also enhances the *in-situ* generation of electrophilic O_{Hads} at the Ni site [Figure 4C]. DFT calculations indicate the optimization of electronic structures for Rh-4d and Ni-3d and the reduction of barriers for electron transfer between active sites towards crucial intermediates HMF and $^*\text{OH}$ [Figure 4D]. Remarkably, the Rh-SA/NiFe NMLDH with a 100% FDCA FE exhibits an excellent long-term stability of more than 100 h (Table 1, entry 5) and great cyclic stability [Figure 4E].

In 2023, Zhou *et al.* described a catalyst consisting of single copper atoms supported on nitrogen-doped carbon nanosheets (Cu/NCNSs) and evaluated its catalytic performance in the electro-oxidation of twelve biomass platform compounds^[68]. The single copper atoms anchored on NCNSs provide numerous active sites, which are significantly distinct from those on the Cu nanoparticles (NPs) in terms of HMF electrooxidation. The mechanism of Cu/NCNSs and Cu NPs in HMFOR is illustrated in Figure 5.

HMF, as an important C_6 biomass derivative, has received wide attention for its catalytic hydrogenation to produce high-value-added products. Wu *et al.* reported a palladium monoatomic electrocatalyst supported

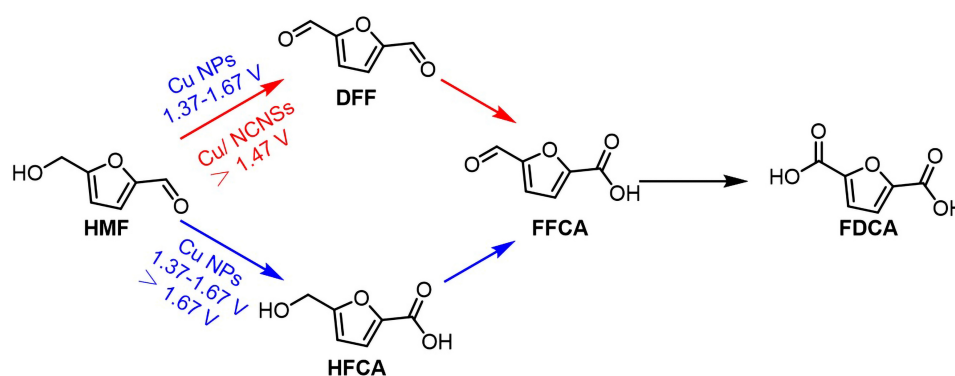


Figure 5. HMFOR mechanism over Cu/NCNSs and Cu NPs.

on TiO_2 for the selective electroreduction of HMF to dimethylfuran (DMF) in a neutral electrolyte [Figure 6A]^[69]. Due to differences in the adsorption configuration of HMF and $^*\text{H}$ coverage, HMF produces bis(hydroxymethyl)hydrofuroin (BHH) on TiO_2 and 2,5-dihydroxymethylfuran (DHMF) on Pd NPs, respectively [Figure 6B and C]. DFT calculation and *in situ* characterization demonstrated that the adjustment of hydrogen spillover and adsorption configuration can influence the selectivity of the product. The presence of Pd single atoms improves the $^*\text{H}$ coverage of TiO_2 surface, promotes hydrogen overflow, and maintains an inclined adsorption configuration, thus improving the selectivity of DMF [Figure 6D].

A ruthenium-copper SAA (Ru_1Cu SAA) catalyst was reported by Ji *et al.*, which achieved efficient electrocatalytic hydrogenation (ECH) of HMF to produce DHMF^[67]. Employing characterization techniques such as HAADF-STEM, X-ray absorption fine structure spectroscopy (XAFS), and CO-adsorption diffuse reflectance infrared Fourier transform spectroscopy (CO-DRIFTS), it was demonstrated that Ru is atomically dispersed on Cu nanowires. At -0.3 V vs. RHE, Ru_1Cu SAA showed a higher DHMF formation rate (0.47 mmol cm^{-2} h^{-1}) and FE (85.6%) (Table 1, entry 6). Moreover, in high HMF concentrations (50 and 100 mM), the FE of Ru_1Cu SAA is significantly higher than Cu, showing its application potential in high concentrations. The authors carried out kinetic studies using techniques such as CV, *in situ* electrochemical impedance spectroscopy, and kinetic isotope effects (KIE) to investigate the kinetics of HMF electrochemical reduction on Ru_1Cu and Cu catalysts. They observed different mechanisms for the electrochemical reduction of HMF on Ru_1Cu and Cu. In the case of Ru_1Cu SAA catalyst, with or without the presence of HMF, there was no change in the rate-determining step (RDS) of the hydrogen evolution reaction (HER) and HMF reduction reaction (HMFRR). This suggests that the hydrogenation of HMF on Ru_1Cu follows an electrochemical hydrogenation (ECH) mechanism. On the other hand, when using Cu as a catalyst, the RDS changes before and after the introduction of HMF. Combining this observation with relevant literature, the researchers proposed that on Cu, the RDS involves a proton-electron coupled transfer (CPET) process, and the reaction mechanism for HMF on Cu is an electroreduction mechanism. Based on the aforementioned analysis, the electrochemical reduction processes of HMF on Ru_1Cu and Cu are proposed, as shown in Figure 6E and F, respectively.

Electrocatalytic upgrading of furfural

FUR, an essential component of hemicellulose, is considered one of the most promising biomass-derived molecules for the production of various fuels and high-value-added chemicals (including furfuryl alcohol, 2-MF, *etc.*) by thermal catalytic hydrogenation. However, traditional thermal reduction methods have some disadvantages, including the use of explosive hydrogen gas or toxic reducing agents and the requirement for high-temperature conditions. Compared to thermal catalytic hydrogenation, ECH offers the advantages of

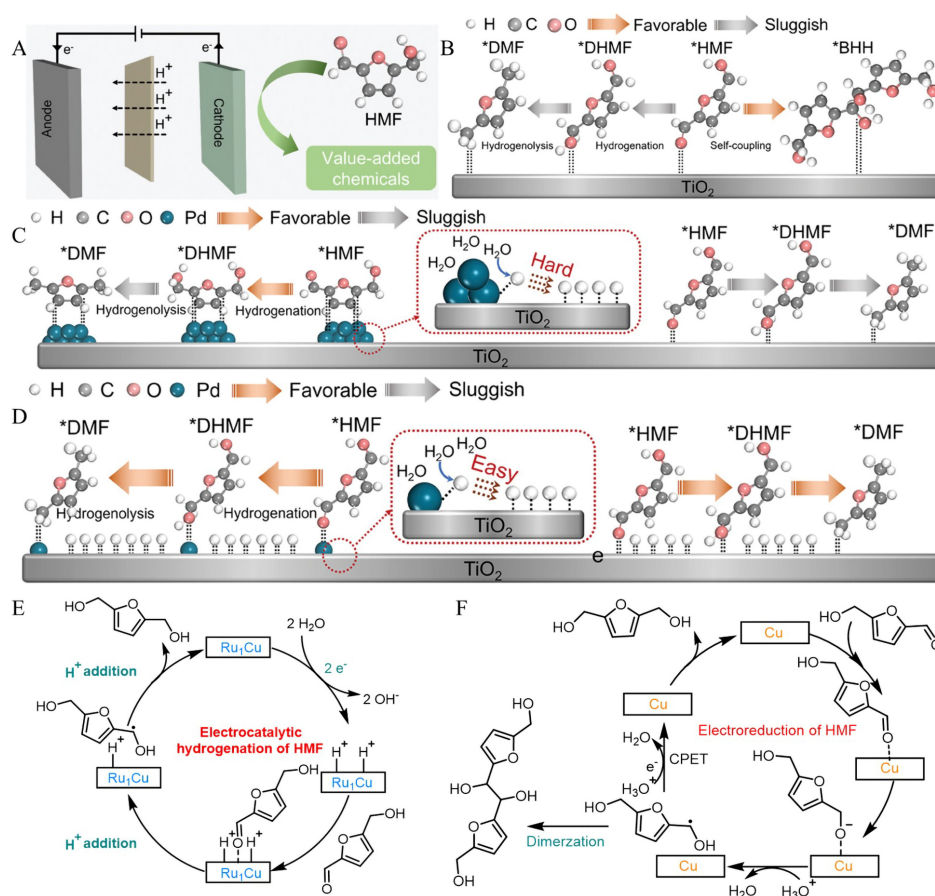


Figure 6. (A) Schematic illustration of electrochemical hydrogenation of HMF. Schematic illustration of the HMFRR process on (B) TiO₂, (C) Pd NPs/TiO₂, and (D) Pd SA/TiO₂. Copyright 2023, Elsevier^[69]. The electrochemical reduction processes of HMF on (E) Ru₁Cu and (F) Cu.

mild reaction conditions, low energy consumption, and sustainability, providing a sustainable alternative for FUR reduction to MF.

Zhou *et al.* reported highly selective ECH of FUR under neutral conditions by P-doped carbon-supported Cu SACs^[70]. The controlled experiments demonstrated that the single-atom Cu site served as the active center for the reaction, facilitating the highly selective hydrogenation of FUR while inhibiting the HER. Additionally, the doping of oxyphilic P enhanced the adsorption of furfuryl alcohol, which promotes the conversion of FUR to 2-MF through furfuryl alcohol intermediates. Through experimental investigations and DFT calculations, Mukadam *et al.* revealed that the adsorption strength of FUR on catalytic active sites plays a crucial role in determining its product selectivity^[71]. They achieved the highly selective synthesis of hydrofuroin by utilizing CuPc and CoPc with weak adsorption capabilities.

The upgrading of polyol

The polyol, such as glucose, glycerol, and ethylene glycol (EG), is widespread in the composition of biomass derivatives. Therefore, enhancing the upgrade of polyols holds significant importance in realizing the utilization of biomass resources and enhancing economic benefits [Table 2].

Table 2. Various SACs for the conversion of polyol

Entry	Polyol	Catalyst	Catalytic activity	Ref.
1	Glycerol	Bi-Co ₃ O ₄	97.05 ± 2.55% FE, 97.01 ± 1.73% formate selectivity	[72]
2	Glycerol	Pt _{5A} -NiCo LDH/NF	85% glycerol conversion, 88.7% FE of formate	[73]
3	Glycerol	Pt-SA/WO _x	60.2% DHA selectivity	[74]
4	Glucose	Pt/def-TiO ₂ NRAs	84.3% gluconic acid yield	[75]
5	Ethylene glycol	PtSAC/TiO ₂	99.7% FE	[76]
6	Ethylene glycol	Pd-N ₄ /Cu-N ₄	Glycolate selectivity (> 88%)	[77]

Electrocatalytic and photoelectrocatalytic upgrading of glycerol and glucose

Doped spinel oxides, such as transition metal single-atom-doped Co₃O₄ catalysts, demonstrate enhanced glycerol oxidation reaction (GOR) activity. The strategy of doping single-atom bismuth (Bi) at the Co_{Oh}³⁺ sites to enhance the selectivity and activity of Co₃O₄ in electrocatalytic GOR was provided by Wang *et al.* in 2022^[72]. The Co(OH)₂ precursor was initially synthesized via electrodeposition, followed by ion exchange in an EG solution containing bismuth nitrate. Subsequently, the Bi-doped Co₃O₄ nanosheet array (Bi-Co₃O₄) was fabricated through a calcination process [Figure 7A]. The AC HAADF-STEM maps of various regions indicate that Bi exists as individual atoms within Bi-Co₃O₄ and is doped into the Oh site of Co₃O₄. Experimental and theoretical studies demonstrate that the substitution of Bi single atoms at Co_{Oh}³⁺ sites facilitates OH* generation at the adjacent Co_{Td}²⁺ sites, leading to a decrease in OH* formation energy on Co₃O₄, thereby enhancing the GOR activity via direct oxidation [Figure 7B and C]. The LSV results show that the incorporation of Bi enhances oxidation activity at lower potentials [Figure 7D]. In the voltage range of 1.25 to 1.65 V *vs.* RHE, Bi-Co₃O₄ exhibits a higher FE for formate compared to Co₃O₄ [Figure 7E]. In particular, at 1.35 V *vs.* RHE, the Bi-Co₃O₄ catalyst demonstrates maximum values of FE and formate selectivity, reaching 97.05 ± 2.55% and 97.01 ± 1.73% (Table 2, entry 1), respectively, while exhibiting excellent stability [Figure 7F].

A general synthesis scheme for a single atom electrocatalyst by a simple condensing-carbonization process was reported by Chen *et al.* in 2020. The prepared SACs exhibited excellent performance of electrocatalytic GOR in an alkaline solution^[78].

LDHs with high specific surface area and abundant defect sites are good carrier materials for the confinement of single metal atoms. In LDHs, oxygen atoms can form M-O bonds with noble metal single atoms, thereby regulating the d-electronic state of precious metal and enhancing chemisorption and activation of reactive substances. Yu *et al.* reported a Pt (5.64 wt%) SAC supported on a NiCo LDH for the conversion of glycerol^[73]. The catalysts were prepared using electrochemical deposition, and Pt single atoms were uniformly distributed on PtSA-NiCo LDH/nickel foam (NF) [Figure 8A and B]. The electron paramagnetic resonance (EPR) spectra have confirmed that Pt increases the concentration of oxygen vacancies [Figure 8C]. The Pt single atoms were suggested to reduce the energy barrier and promote catalytic performance. According to DFT calculations, incorporating single-atom Pt doping can result in a downward shift of the d-band center [Figure 8D]. Under optimized conditions (1.375 V *vs.* RHE), the SAC led to an 85% glycerol conversion with an 88.7% FE of formate [Figure 8E and F] (Table 2, entry 2). A minor presence of carbonate was identified via ¹³C nuclear magnetic resonance (NMR), suggesting ongoing oxidation of formate to carbon dioxide [Figure 8G]. Based on this, the oxidation mechanism of glycerol was proposed [Figure 8H]. The main reaction pathway for the glycerol ECO to formic acid is as follows: glycerol is oxidized to glycerol aldehyde at the anode, which is further oxidized to glyceric acid. Subsequently, carbon-carbon bonds cleave to yield acetic acid and formic acid. Simultaneously, acetic acid can be further oxidized to produce acetaldehyde, which then undergoes carbon-carbon bond cleavage to generate two

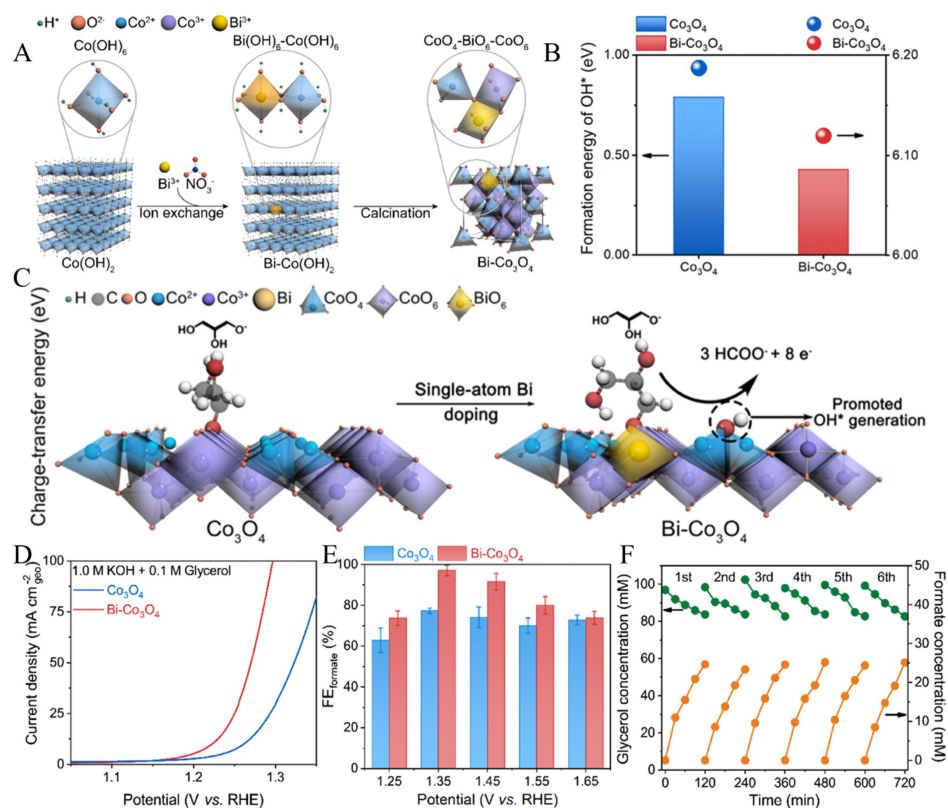


Figure 7. (A) The synthesis for Bi-Co₃O₄. (B) Formation energies of OH* and charge-transfer energies of Co₃O₄ and Bi-Co₃O₄. (C) The influence of Bi doping on the co-adsorption of OH* and glycerol. (D) LSV curves of Co₃O₄ and Bi-Co₃O₄. (E) The FE at wide potential range. (F) Stability test of Bi-Co₃O₄. Copyright 2022, ACS^[72].

molecules of formic acid.

Photoelectric chemical (PEC) biomass conversion is considered as a promising technology that can transform renewable energy into high-value-added products. Among many conversion reactions, the oxidation of glycerol by PEC to dihydroxyacetone (DHA) is considered to be a promising method. A WO₃ amorphous/crystalline homojunction photoanode doped with Pt single atoms (Pt-SA/WO₃) has been successfully constructed by Feng *et al.* in 2024, showing excellent GOR performance in acidic solution, with 60.2% selectivity of DHA at 1.2 V vs. RHE (Table 2, entry 3)^[74]. In addition, experimental and DFT calculations show that the synergistic effect of vacancies and single-atomic doping can accelerate the charge transfer rate, prolong the carrier lifetime, and reduce the GOR kinetic barrier, thereby improving the activity of GOR and selectivity of DHA. Ensuring the sustainability of photoanodes is essential for practical applications of photoelectrocatalysis. While the photocurrent density of WO₃ decreases rapidly to 39.9% of its initial value after five hours of PEC processing, indicating inadequate stability, the photocurrent densities of WO_x and Pt-SA/WO_x remain at 59.0% and 68.6% of their initial values, respectively. This demonstrates that incorporating amorphous/crystalline homojunction and Pt single-atom sites benefits photoanode stability.

In 2023, Tian *et al.* reported a photoelectrochemical method that employs a defective TiO₂ nanoarray for the immobilization of a single-atom platinum (Pt/def-TiO₂ NRAs) as a photoanode, enabling selective oxidation of glucose and its conversion into high-value-added gluconic acid^[75]. The defect structure caused

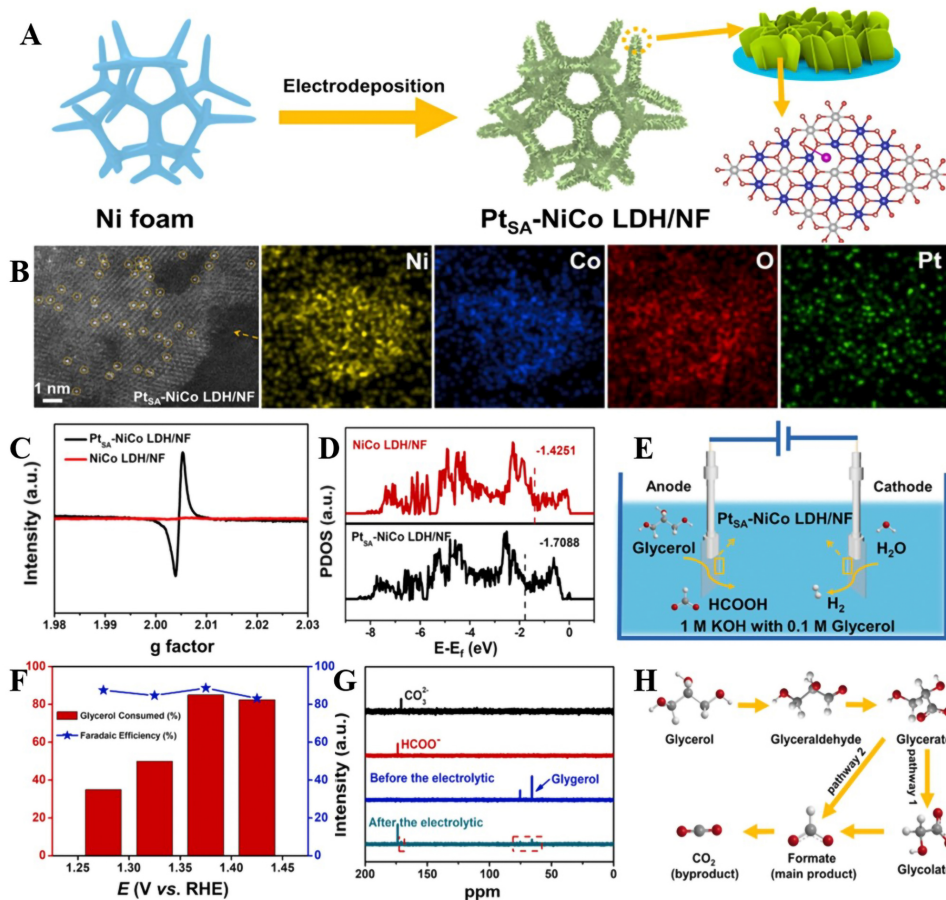


Figure 8. (A) Schematic illustration for the fabrication, (B) AC HAADF-STEM and EDX element mapping images of Pt_{SA}-NiCo LDH/NF. (C) EPR spectra, (D) PDOS patterns of Pt_{SA}-NiCo LDH/NF and NiCo LDH/NF. (E) The schematic illustration of HER/GOR. (F) Electrolytic performance across a wide potential range. (G) The ¹³C NMR spectra of CO₃²⁻, HCOOH, and the electrolyte before and after the reaction, (H) Schematic diagram of glycerol oxidation mechanism. Copyright 2023, Elsevier^[73].

by oxygen vacancy can regulate both carrier dynamics and band structure. After the optimization of oxygen vacancy, the charge separation rate of Pt/def-TiO₂ NRAs significantly improved the selectivity and yield of C₆ products, and realized the selective oxidation of glucose to gluconic acid. In this study, the optical flux density of glucose oxidation by Pt/def-TiO₂ NRAs at 0.6 V was 1.91 mA cm⁻², and the yield of gluconic acid under simulated sunlight irradiation was 84.3% (Table 2, entry 4). In the electrooxidation of glucose, the stability of Pt/def-TiO₂ photoanodes was investigated through five cycles of J-t experiments. The electrolyte was replaced every 5.5 h, and after 27.5 h of testing, no significant decay of photocurrent densities for glucose was observed, indicating excellent stability of the Pt/def-TiO₂ photoanode.

Electrocatalytic upgrading of ethylene glycol

EG is a diol produced by the hydrogenation of cellulose. Due to its non-toxic, higher energy density, high boiling point, and good reactivity, it is considered a promising renewable material for the production of value-added chemicals such as formates and glycolates.

Ayele *et al.* pioneered the synthesis of Pt single atoms supported on titanium oxide (PtSAC/TiO₂) for EG oxidation (EGO)^[76]. PtSAC/TiO₂ and PtNP/TiO₂ catalysts were synthesized using a simple, rapid, economical hydrothermal-assisted co-precipitation method. The extended XAFS (EXAFS) analysis provides evidence of Pt single atoms [Figure 9A]. In CV tests, PtSAC/TiO₂ exhibits a high ratio of J_r/J_b , suggesting either reduced adsorption of reaction intermediates of EGO or the synergistic effect of the TiO₂ support in aiding the removal of reaction intermediates from the active sites [Figure 9B]. The PtSAC/TiO₂ catalyst exhibits an outstanding total FE of 99.7% at 0.7 V vs. RHE (Table 2, entry 5), which is higher than that of PtNP/TiO₂. The PtSAC/TiO₂ enhances the electronic interaction between Pt and TiO₂, thereby contributing to improved stability, as evidenced by a minimal decrease in current drop within a 12-h timeframe in an alkaline solution. Subsequently, the same group prepared a Pt SAC supported on Ni-doped TiO₂, which enables the partial oxidation of EG by Ni doping^[79]. The catalyst containing Ni establishes an environment that facilitates enhanced OH⁻ adsorption, enabling increased accessibility of Pt for subsequent oxidations. Additionally, the catalyst exhibits exceptional FE (> 98%) and stability in the alkaline environment during the EGO. The catalyst exhibits enhanced electrocatalytic performance in the oxidation of EG, attributed to the synergistic effects of Ni and Pt, as depicted in Figure 9C and D. The strong interactions between the substrate and the catalyst prevent the aggregation of single atoms, thereby improving stability. Incorporating secondary metal atoms has the potential to enhance the activity of SACs. It is logical to anticipate that the interplay of the electronic structures of two metal elements will lead to a more optimized configuration, facilitating the attainment of an appropriate state for the adsorption and desorption of intermediate reactions. Consequently, dual-site SACs (DSACs) empower diatomic sites to exhibit superior catalytic activity compared to their isolated single.

In 2022, Moges *et al.* utilized copper phthalocyanine as the precursor and successfully synthesized DSACs Pd-N₄/Cu-N₄ through a simple, economical, high metal loading, and efficient electrochemical reduction [Figure 10A]^[77]. This provides an efficient and environmentally friendly strategy for synthesizing DSACs, suitable for diverse reactions. Energy dispersive X-ray Spectroscopy (EDX) in the STEM revealed a uniform distribution of Pd, Cu, C, and N on the exposed surface of the electrode [Figure 10B].

Because of the higher atomic number of Pd compared to Cu, Pd in the HAADF-STEM image displays a greater number of bright spots than Cu [Figure 10C and D]. Fourier-transformed EXAFS (FT-EXAFS) analysis showed that no Pd-Pd bonds were observed in the Pd-N₄/Cu-N₄ catalyst. These results serve to validate the existence of Pd and Cu in a singular atomic form, evenly dispersed across the exposed surface of the electrode. Furthermore, according to the X-ray absorption spectroscopy (XAS) and XPS analyses, the oxidation state of Pd in Pd-N₄/Cu-N₄ was determined to be +2. The findings demonstrate that Cu within Pd-N₄/Cu-N₄ exists in both +1 and +2 oxidation states [Figure 10E and F]. In alkaline media, the mechanism of EGO on DSAC Pd-N₄/Cu-N₄ electrocatalysts can be delineated into two consecutive steps: initially, EGO yields glycolate, followed by its further oxidation to formate. Remarkably, glycolate was identified as the primary product of EGO on the Pd-N₄/Cu-N₄ electrocatalyst. This is attributed to the synergistic effect of Pd and Cu single atoms, facilitating EGO in alkaline environments. Surface Cu species are enveloped by OH⁻ ions, facilitating electron transfer to Pd atoms. The electron-rich Pd atoms, in turn, enhance the catalytic ability of Pd species to suppress C-C bond cleavage. Outperforming various palladium-based electrocatalysts reported in the literature, the Pd-N₄/Cu-N₄ electrocatalyst demonstrates significantly higher glycolate selectivity (> 88%) (Table 2, entry 6).

The upgrading of ethanol

Bioethanol is a form of renewable energy generated through the fermentation of biomass or agricultural waste. In recent years, there has been widespread attention directed towards the ethanol oxidation reaction (EOR), propelled by the significance of bioethanol and its integral role in addressing energy demands and

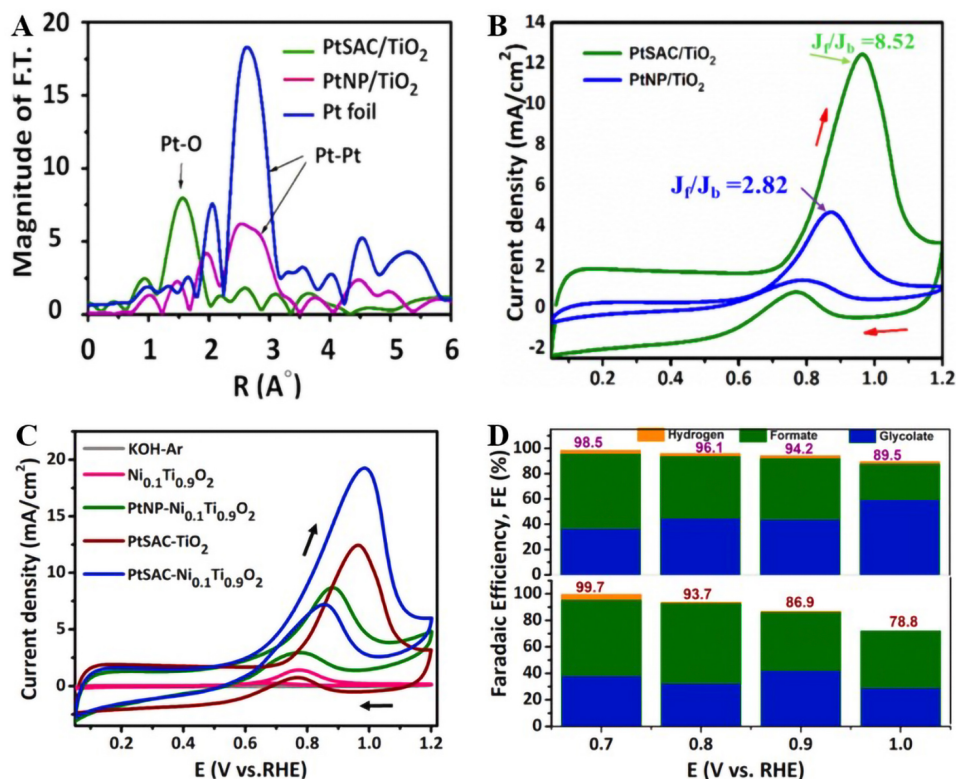


Figure 9. (A) FT-EXAFS spectra, (B) the J_f/J_b of PtSAC/TiO₂ and PtNP/TiO₂. Copyright 2022, Elsevier^[76]. Comparison of (C) catalytic activity and (D) FE and product distribution of PtSAC-Ni_{0.1}Ti_{0.9}O₂ (top) and PtSAC-TiO₂ (bottom). Copyright 2023, Elsevier^[79].

environmental cleanliness. Its applications span various sectors, including but not limited to fuel, fuel additives, and disinfectants. Direct ethanol fuel cells (DEFCs) have the prospect of large-scale application due to their advantages (e.g., relatively convenient transportation and storage, security) of ethanol. EOR can proceed via two parallel pathways: complete oxidation and partial oxidation. The complete electrooxidation of ethanol (C₁ pathway) with the formation of CO₂ by breaking the C-C bond and the product of incomplete oxidation (C₂ pathway) is acetate. CH₃CHO is a typical intermediate of ethanol oxidation. However, the low selectivity of the C₁ pathway restricts the efficiency of ethanol's complete oxidation. Developing efficient and durable electrocatalysts is crucial for the commercial viability of DEFCs. While noble metals, such as Pt and Pd, demonstrate exceptional performance in ethanol electrooxidation, their high cost, limited availability, and susceptibility to CO poisoning hinder widespread deployment. SACs, as highly efficient catalysts with nearly 100% atomic utilization, have been widely applied in bioethanol electrooxidation. Furthermore, SAA catalysts have been engineered to enhance stability.

In 2016, Liu *et al.* reported on how to precisely manipulate and control the atomic geometry of Pd shell atoms on Au nanowires, thereby achieving the formation of isolated and continuous Pd atoms on the surface of these nanowires^[80]. However, various results lead to the same conclusion that Pd ensembles, rather than single Pd atoms, serve as the active sites for EOR. In 2020, Tiwari *et al.* reported that Pd-Co₂P-PdSAs@GO (palladium-cobalt phosphide NPs with Pd single atoms anchored on graphene oxide) catalysts showed high activity in EOR, with a mass activity (MA) of 10,520 mA mg_{Pd}⁻¹, which is remarkably more significant than Pt/C^[81]. Pd-Co₂P-PdSAs@GO exhibits high catalytic activities, C₁ pathway selectivity and stability in alkaline electrolytes. The promotion of catalyst activities is attributed to charge transfer between Pd single atoms and Co₂P to shift the Pd d-band center, and the distinctive electronic configuration of

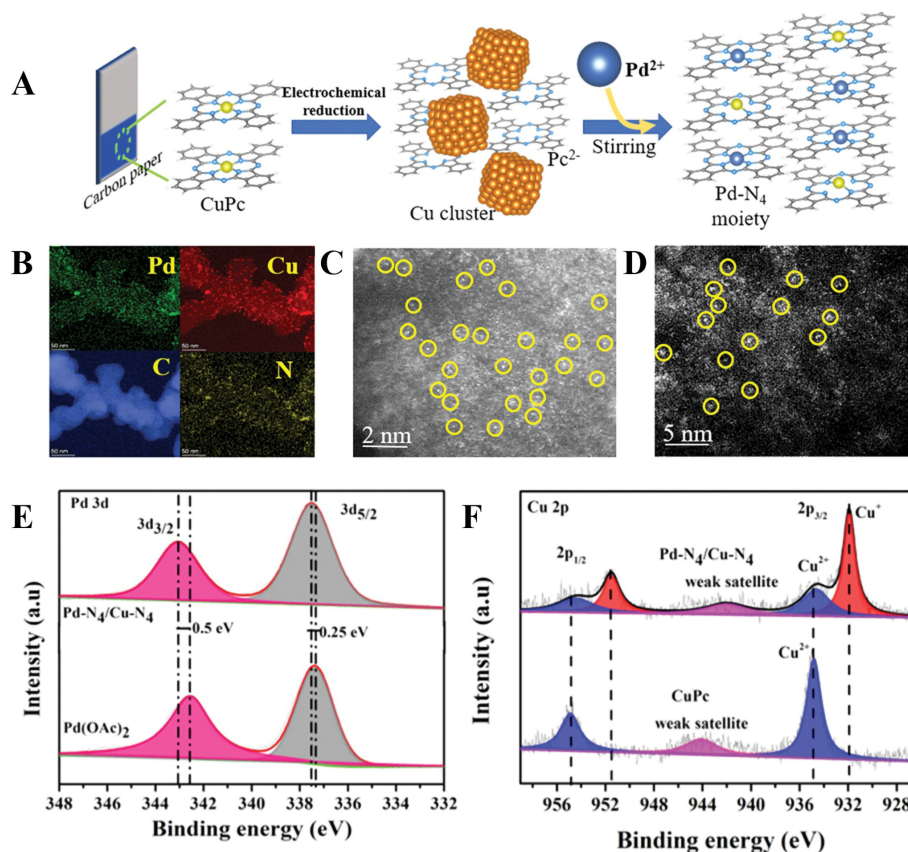


Figure 10. (A) The synthesis of Pd-N₄/Cu-N₄ by electrochemical reduction. (B) The EDX mapping images of C, N, Pd, and Cu. Aberration-Corrected HAADF-STEM images of Pd-N₄/Cu-N₄ showing the distribution of (C) Pd and (D) Cu. (E) Pd 3d for Pd-N₄/Cu-N₄ and Pd(OAc)₂; (F) Cu 2p for CuPc and Pd-N₄/Cu-N₄. Copyright 2020, Wiley^[77].

Pd-N_x (where *x* ranges from 1 to 4) sites increases the conductivity of nitrogen-doped GO. This advancement enables the strategic development of atomically dispersed catalysts, thereby unlocking new avenues for exploration.

Surface modification strategies of noble metal nanocatalysts can adjust the local electronic structure to enhance EOR activity, but usually at the expense of the electrochemically active surface area (ECSA). Hence, the spotlight increasingly falls on SACs. The rapid oxidative removal of CO species at noble metal sites is crucial for enhancing ethanol oxidation activity. Reportedly, Ni SACs provide a substantial quantity of adsorbed OH species, which can facilitate the oxidative elimination of CO at noble metal sites. Therefore, dispersing Ni single atoms onto noble metal NPs may improve the performance of EOR. Single Ni atom-modified Pt nanowires (SANi-PtNWs) developed by Li *et al.* exhibited superior EOR and methanol oxidation reaction (MOR) activity^[82]. The author used inductively coupled plasma atomic emission spectroscopy (ICP-AES) to prove that there should be 2.4 Ni atoms and 15 Pt atoms per square nanometer pair; that is, the ratio of Ni and Pt atoms on the surface is about 1:6. Then, by means of EXAFS and XANES tests in synchrotron radiation, it is shown that Ni atoms are dispersed on the surface of Pt, and the average oxidation state of Ni close to two, consistent with the XPS studies. The MA of SANi-PtNWs ($5.60 \pm 0.27 \text{ A mg}_{\text{Pt}}^{-1}$) was three and seven times higher compared to PtNWs and Pt/C, respectively. A decrease of 61 mV in overpotential suggested the lower barrier of EOR on the SANi-PtNWs surface.

Experiments and DFT calculations show that SANi alters the local atomic configuration and electronic structure of the surrounding Pt atoms, as well as the binding strength of CO, thereby improving the EOR/MOR activity and catalyst durability. Li *et al.* synthesized a Pd NPs catalyst with uniformly dispersed Ni single atoms (Pd NPs@Ni SAC) using a two-step method, which exhibits excellent EOR performance, displaying good C₁ pathway selectivity (28%) and excellent electrocatalytic stability^[83].

Strain engineering can regulate catalytic performance by adjusting the catalyst's electronic structure and intermediates' adsorption energy on the surface. The synergistic effect between tensile strain and the influence of ligands can enhance the activity of EOR. It has been reported that applying tensile strain to Pt increases its surface reactivity towards EOR. Zhang *et al.* designed and synthesized core-shell PtBi@Pt catalyst with Pt subjected to tensile rather than compressive strain, thereby enhancing EOR activity^[84]. Importantly, *in situ* fourier transform infrared spectroscopy (FTIR) analysis reveals that PtBi/SA Pt and Pt/C predominantly follow the C₂ pathway, whereas ethanol undergoes complete oxidation to CO₃²⁻ on PtBi@Pt via the C₁ pathway. Luo *et al.* applied tensile-strained PtBi@PtRh₁ to anodic EOR, where the catalyst was synthesized via atomic galvanic replacement and electrochemical dealloying [Figure 11A]^[85]. The MA of PtBi@PtRh₁ was 70.4, 64.5, and 12.3 times higher than that of PtBi nanoplates, PtBi-3.6% Rh₁ nanoplates, and Pt/C, respectively. The PtBi@PtRh₁ catalyst exhibits higher electrochemical oxidation activity of CH₃CHO and C₁-pathway selectivity of EOR in comparison with Pt/C and PtBi@Pt, suggesting that the synergistic effect between tensile strain Pt and Rh single atoms can promote the cleavage of the C-C bond. Meanwhile, DFT calculation confirmed this conclusion and also demonstrated that this synergistic effect can promote the adsorption of ethanol and intermediates. The Rh-Pt SAA catalysts, however, did not achieve a high selectivity for the C₁ pathway.

In 2022, Zhang *et al.* reported a strategy of constructing single-atom Ir-tensile-strained Pt (100) catalyst at heterophase hcp-PtPb/fcc-Pt core-shell hexagonal nanoplates (PtPb@PtIr₁ HNP/C) to enhance the activity and selectivity of EOR^[86]. The noble metal Ir facilitates C-C bond cleavage in EOR; thus, single-atom Ir sites can be used to enhance the selectivity of the C₁ pathway to promote EOR activity. In Figure 11B, it is evident that the PtPb@PtIr₁ hexagonal nanoplates (HNPs) exhibit a higher selectivity and FE (57.93%) in the complete oxidation of ethanol, showcasing the ability of Ir₁ sites to enhance the selectivity of the C₁ pathway and suppress the formation of acetic acid in EOR. Additionally, the lower onset oxidation potential and higher current density of PtPb@PtIr₁ HNP/C indicate that the EOR activity can be enhanced by incorporating Ir₁ sites. CO-stripping curves suggest that the key sites for the oxidation of COads intermediates are the Pt(110) surface rather than Ir₁ [Figure 11C]. Meanwhile, the tolerance of CO intermediates of PtPd@PtIr₁ HNPs is superior to that of Pt/C.

Zhang *et al.* found that hydrogen implantation can induce tensile strain and cause the D-band center of Pd to downshift^[87]. Experiments and DFT calculations indicate that H-implantation can enhance the p-d orbital hybrid interaction between Ga and Pd, thereby significantly promoting the C-C bond cleavage and CO* oxidation in the C₁ pathway, showing excellent EOR activity and C₁ pathway selectivity [Figure 11D and E].

The Rh-based catalyst has been verified to effectively catalyze the conversion of ethanol into CO₂ via the C₁ pathway^[88,89]. Although PtBi@PtRh₁ catalyst synthesized by Luo *et al.* can promote C-C bond breaking, the C₁ pathway is not highly selective^[85]. In 2022, Chang *et al.* utilized a two-step solution method to synthesize partially oxidized single Rh dispersed on the (100) surface of Pt nanocubes (Rh_{at}O-Pt NCs), which shows an unprecedentedly high CO₂ selectivity with low CO₂ generation potential compared to other Pt-based electrocatalysts in the EOR literature^[90]. Experiment and DFT calculations demonstrated that the Rh

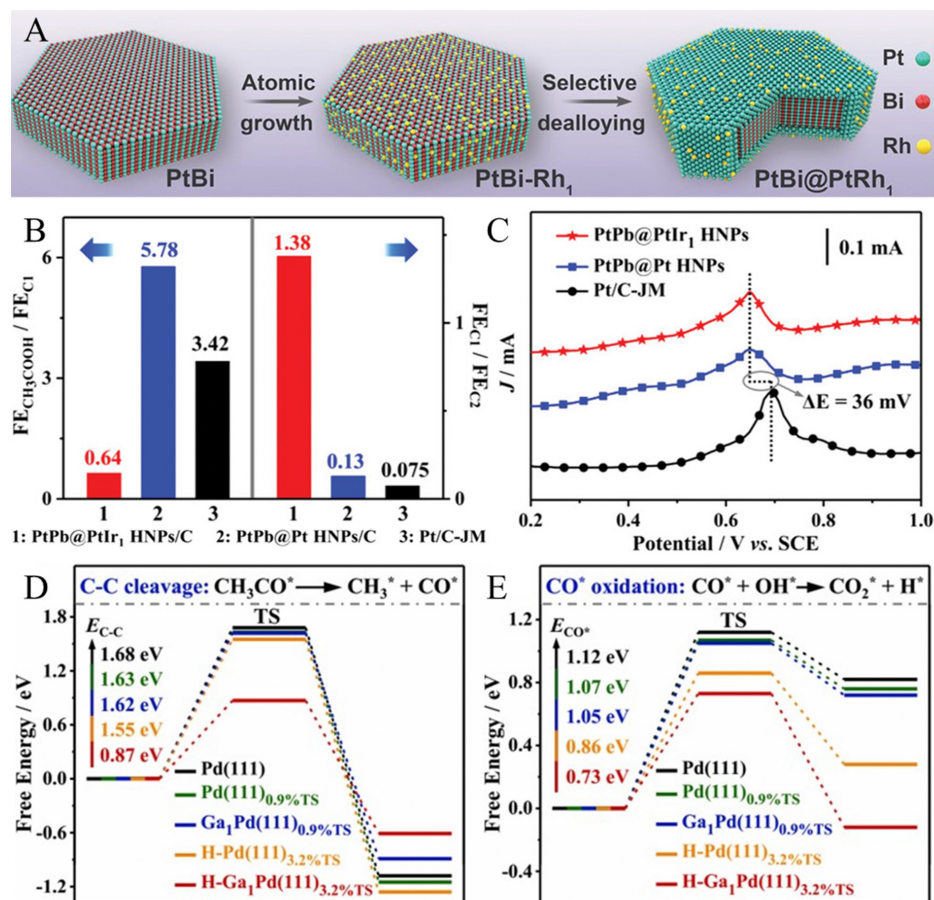


Figure 11. (A) Schematic illustration of the preparation procedure of PtBi-3.6% Rh₁ and PtBi@PtRh₁ nanoplates. Copyright 2021, Wiley^[85]. (B) FE_{CH₃COOH}/FE_{C1} and FE_{C1}/FE_{C2}. (C) CO-stripping curves of the three catalysts. Copyright 2022, Wiley^[86]. Reaction energy barriers for (E) C-C bond cleavage of CH₃CO* and (F) CO* oxidation. Copyright 2024, Elsevier^[87].

decoration remarkably improved the CO₂ selectivity in EOR, but the role of Rh and Pt in improving the performance of EOR is different, with Rh promoting the cleavage of C-C bond to form *CH₃ + *CO intermediates and the removal of *CO intermediates, while Pt as the active center of the overall EOR activity [Figure 12A and B]. The Rh_{at}O-Pt NCs/C catalyst has a strong ability to break the ethanol C-C bond in the range of 0.35 to 0.75 V vs. RHE, and the selectivity of CO₂ reaches 99.9% [Figure 12C].

Pei *et al.* prepared a multimetallic catalyst, where Pd nanoclusters and Ru single atoms were anchored onto defect sites of Ni(OH)₂^[91]. The interaction between neighboring Ru and Pd, along with the adsorption of OH_{ad} by Ni(OH)₂ at low potential, results in the reduction of the reaction barrier for eliminating reactant intermediates and improves the selectivity of the C₁ pathway in the EOR process. Wang *et al.* developed an efficient PdBi SAA catalyst (ionic liquid (IL)/Pd₅₀Bi₁) by manipulating noble metal aerogel at the atomic scale, utilizing a one-step NaBH₄ reduction method, and applied it in EOR^[92]. The introduction of Bi single atoms increased the catalyst's surface area, providing more abundant active sites, accelerating electron and mass transfer rates, and enhancing ethanol oxidation activity. Due to the introduction of single atom Bi and the interface engineering between the surface and IL, the IL/Pd₅₀Bi₁ aerogel demonstrated excellent ethanol oxidation performance. The MA of IL/Pd₅₀Bi₁ aerogel was 4.1 times higher than that of Pd/C catalyst. Furthermore, the IL/Pd₅₀Bi₁ aerogel has superior performance compared to currently reported Pd-based nanomaterials, exhibited excellent stability, higher CO tolerance, and faster charge transfer efficiency. NMR

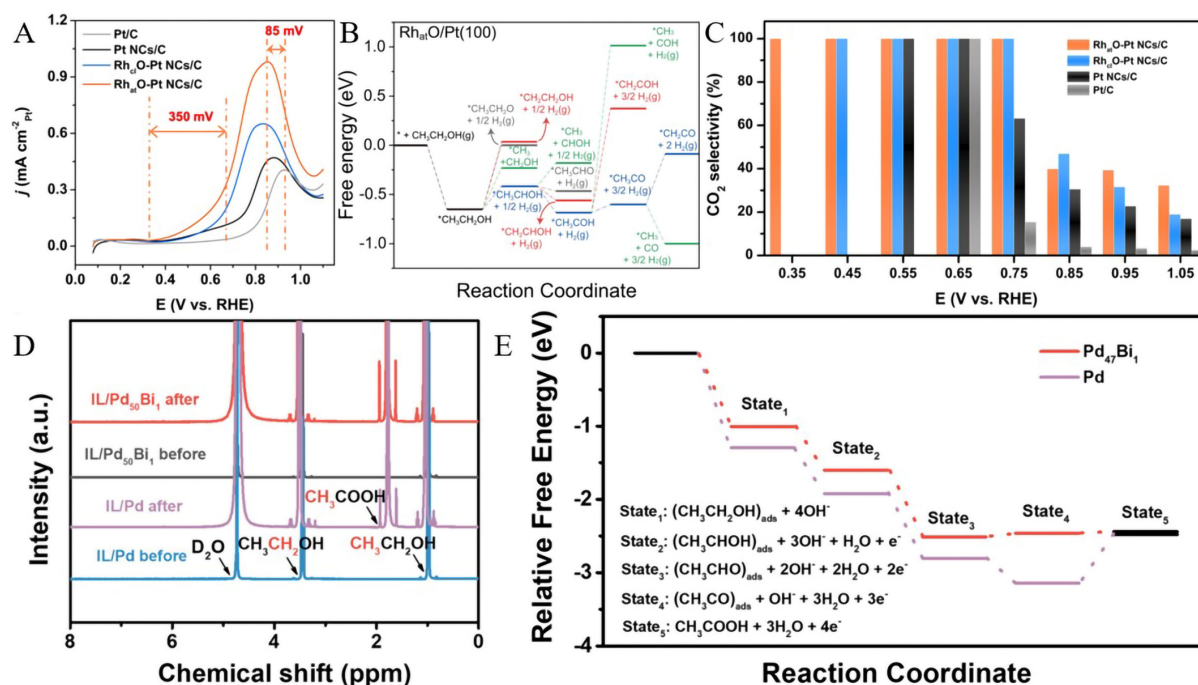


Figure 12. (A) Anodic polarization curves for electrocatalysts. (B) DFT-calculated free energy profile of C-C bond cleavage of CH₃CH₂OH on Rh₃O₄/Pt(100). (C) The CO₂ selectivity of all samples. Copyright 2021, Elsevier^[90]. (D) Analysis of the electrolytes by 1H NMR before and after EOR. (E) The free energy for the EOR. Copyright 2021, Wiley^[91].

analysis of the electrolyte before and after ethanol oxidation electrolysis revealed that Bi significantly improved the selectivity toward the C₂ pathway [Figure 12D]. DFT calculations also confirmed the reduction of the energy barrier of the RDS with the introduction of Bi single atoms, thereby accelerating the reaction kinetics of EOR [Figure 12E].

The upgrading of methanol

Methanol, the simplest primary alcohol, can be derived from biomass and has increasingly emerged as a favored chemical feedstock due to its wide availability and low cost. Although Pt-based catalysts demonstrate remarkable catalytic activity in the MOR, their high cost, limited availability, and susceptibility to CO poisoning hinder their widespread application in MOR. Therefore, the utilization of single-atom Pt catalysts to reduce Pt usage, along with the development of efficient, CO-tolerant Pt-based catalysts, holds significant importance for enhancing their durability and MOR activity. However, researchers have observed that the CO pathway for methanol oxidation cannot be facilitated on single Pt atoms due to the strong binding of CO intermediates to Pt sites. It has been reported that Pt SACs supported on carbon black and carbon nanotubes (CNTs) exhibit negligible activity towards MOR.

Zhang *et al.* employed a facile adsorption-impregnation method to prepare two types of Pt SACs, Pt₁/RuO₂ and Pt₁/VXC-72, using RuO₂ and carbon black as substrates, respectively^[93]. Pt₁/RuO₂ SACs exhibited excellent MA, remarkable catalytic stability, and high tolerance to CO poisoning. However, the single-atom Pt on carbon black showed inappreciable MOR activity, consistent with literature reports. Experimental and DFT calculations showed that the coordination environment of Pt single atoms changed with RuO₂ substrate, enhancing both the stability and MOR activity of Pt₁/RuO₂ through facilitated electrochemical CO removal. In 2022, Poerwoprajitno *et al.* synthesized single-Pt-atom-on-Ru catalysts, with individual Pt atoms supported on low-index facets of Ru NPs, for MOR^[94]. The strong Pt-Ru bond is a key factor in

maintaining structural stability during catalysis. Additionally, DFT calculations demonstrated that the catalyst exhibits strong methanol adsorption and weak CO binding capability, thus favorably augmenting MOR activity.

Chen *et al.* developed a high-performance Pt-based SAA catalyst ($\text{Ru}_1\text{Pt}_n\text{-SAA}$) for MOR through the dual modulation of H_2 and NO^{3-} [95]. Control experiments indicated that $\text{Ru}_1\text{Pt}_n\text{-SAA}$ could not be successfully synthesized in the absence of either NO^{3-} or H_2 . XAFS and XPS results showed that Pt exists in a metallic state, with electrons transferring from Ru to Pt, and the absence of Ru-Ru bonds confirmed the singular atomic form of Ru within $\text{Ru}_1\text{Pt}_n\text{-SAA}$. DFT calculations demonstrated that the introduction of Ru into Pt NPs decreases the reaction free energy of the RDS ($\text{CO}^* + \text{OH}^*$) in MOR. This facilitates easier activation of water molecules on the surface of $\text{Ru}_1\text{Pt}_n\text{-SAA}$ and reduces the binding energy of Pt with CO, making CO desorption easier and enhancing MOR activity. Kong *et al.* prepared Ru-ca-PtNi catalysts for OER and unveiled a single-atom-cavity coupling mechanism, which enhances the activity and stability of SACs[96]. The MA of Ru-ca-PtNi was 5.8 times higher than Pt/C. Electrochemical *in situ* IR spectroscopy reveals that Ru single atoms anchored to vacancies can accelerate the desorption of CO. Experimental and DFT calculations indicate that single atom-vacancy coupling can regulate the electronic structure of Pt and optimize the position of the d-band center to promote the MOR. Zhuang *et al.* synthesized a highly efficient catalyst for methanol oxidation, denoted as $\text{Pd}_{\text{NPs}}/\text{Pd-N}_x\text{@C}$, by integrating Pd single atoms and NPs on nitrogen-doped carbon (N-C) substrates, which demonstrated superior MOR activity and stability[97]. Analysis of the ratio between forward and backward peak current densities, along with the CO stripping voltammogram, suggested that CO was more effectively oxidized and removed on the $\text{Pd}_{\text{NPs}}/\text{Pd-N}_x\text{@C}$ catalyst. Experimental investigations and DFT calculations revealed that charge transfer is identified as pivotal in influencing the binding strength between active sites and CO intermediates. Specifically, the preferential electron transfer from Pd single atoms to the support hindered the charge transfer between Pd NPs and the support, thus enhancing the MOR activity and stability of the catalyst. Ruan *et al.* introduced Pt NPs onto N-C-supported Co single atoms via a two-step method, where the synergistic effect between N-C, Co single atoms and Pt NPs enhanced the resistance to CO poisoning and MOR activity[98]. Specifically, Co single atoms facilitated the oxidation and removal of CO intermediates on Pt NPs, and improved CO tolerance, while the N-C support promoted charge transfer and inhibited Pt NP aggregation. Additionally, owing to the excellent oxidation and removal capability of CO intermediates, the catalyst is made suitable for ethanol and formic acid electrooxidation. Ruan *et al.* prepared a novel methanol oxidation catalyst by loading iron single atoms onto graphitic carbon nitride ($\text{Fe/g-C}_3\text{N}_4$) [99]. This catalyst exhibits strong adsorption capability towards methanol and the methanol oxidation process was investigated through DFT calculations.

In addition, the single-atom modification of Pt and Pd becomes a highly efficient strategy to improve catalytic performance, triggering the largest number of active sites. Through etching and annealing treatments, Fan *et al.* harnessed the inherently isolated Bi atoms within Pt-Bi intermetallic compounds to fabricate surface-enriched single Bi atom-modulated Pt nanorods for MOR[100]. The MA of SE-Bi₁/Pt NRs achieved $23.77 \text{ A mg}_{\text{Pt}}^{-1}$, surpassing that of commercial Pt/C by 12.8 times. Experimental and DFT calculations corroborate that surface-enriched Bi single atoms facilitated the CO-free pathway and expedited the kinetics of $^*\text{HCOOH}$ formation. Wei *et al.* found that doping Ir single atoms onto Pd NPs can enhance CO tolerance and increase MOR activity and stability[101]. Electrochemical tests showed that the catalyst exhibits a MOR MA of approximately $1,717.3 \text{ mA mg}_{\text{Pd}}^{-1}$. DFT calculations demonstrate that Ir single atoms alter the electronic structure of Pd NPs, facilitating electron transfer from Pd to Ir, thus contributing to the superior performance observed.

SACS FOR THE UPGRADING OF LIGNIN

Lignin, the most abundant aromatic polymer in nature, is a rich source of renewable energy due to its high calorific value and aromatic content. It is a complex cross-linked macromolecule composed of numerous aromatic rings interconnected by C-O-C and C-C bonds, exhibiting a complex structure and low reactivity. Lignin can be processed to produce various high-value fuels, chemical feedstocks, and pharmaceutical intermediates. In recent years, lignin conversion has emerged as a forefront research area worldwide. Among various lignin conversion technologies, traditional thermochemical treatments have been the most mature and extensively studied. However, their harsh reaction conditions limit their large-scale application and hinder green and sustainable production. With the advancement of green chemistry, electrocatalytic lignin conversion has gained considerable attention due to its mild reaction conditions, offering new green catalytic strategies for lignin conversion research.

The key to realizing the lignin valorization to harvest high-value-added aromatic compounds is selective cleavage of C-C bonds. Miao *et al.* prepared Ir-NiFeO@NF catalyst via hydrothermal and impregnation methods, which realized the upgrading of lignocellulose and energy-saving hydrogen production^[102]. When 1-phenylethanol was used as a substrate, benzoic acid was obtained with a yield of 91.4%. DFT calculations suggest that individual Ir atoms promote the adsorption of reactants and the generation of OH* to facilitate the cleavage of C(O)-C bonds. Cui *et al.* successfully prepared a nitrogen-doped layered porous CNT carrier using the copolymerization reaction of aniline and pyrrole, and carbonization, and further impregnated in chloroplatinic acid to obtain Pt₁/N-CNTs catalyst^[103]. Characterization through EDX-mapping, aberration-corrected STEM (AC-STEM), and EXAFS revealed that Pt exists in a single-atom dispersed state. EXAFS spectrum fitting indicated that the central atom adopts a Pt-N₄ coordination structure. At room temperature, the yield of benzaldehyde reached up to 81% in the ECO cleavage reaction of 2-Phenoxy-1-phenylethanol, significantly higher than commercial Pt/C. A series of control experiments, including radical trapping and isotope labeling experiments, demonstrated that the reaction mechanism of the Pt₁/N-CNTs catalyst differs from that of traditional catalysts. The reaction proceeds through a radical pathway, with the RDS being C_β-H abstraction. The exceptional activity of Pt₁/N-CNTs stems from the Pt-N₃C₁ sites, which facilitate the formation of crucial C_β radical intermediates. These enable the selective cleavage of the C_α-C_β bond to obtain benzaldehyde. Through systematic experimental studies and DFT calculations, two possible reaction mechanisms were proposed by the authors [Figure 13A]. Initially, tert-butyl hydroperoxide (TBHP) is oxidized at the anode, resulting in the generation of tert-butyl radical (A₁·, Pathway 1) and tert-butyl peroxide radical (A₂·, Pathway 2). Subsequently, radical intermediate B· is generated from 2-Phenoxy-1-phenylethanol. Intermediates C₁ and C₂ are then formed through radical/radical cross-coupling. Finally, the selective cleavage of the C_α-C_β bond yields benzaldehyde, CO₂, and other products. Recently, ECH has garnered considerable attention due to its environmentally benign and mild approach. The key factor to improve the FE is the modulation of substrate and hydrogen adsorption energy on the cathodic catalyst surface to prevent the occurrence of HER. Tong *et al.* reported an electrocatalyst comprising Pt single atoms supported on a CoO/Co heterostructure (Pt₁-CoO/Co), investigating the ECH performance of lignin derivatives using phenol as a model substrate^[104]. DFT calculations and experimental studies demonstrated that the synergistic effect of Pt₁-CoO/Co improves the ECH activity of phenol. The Pt atoms anchored around metallic Co facilitate proton reduction and adsorption, while CoO sites adsorb and activate phenol. Subsequently, hydrogen adsorbed on the single Pt atoms is transferred to the activated phenol, enabling the efficient ECH of phenol to yield high-value KA oil while simultaneously inhibiting the HER [Figure 13B].

CONCLUSIONS AND PERSPECTIVE

Biomass, a crucial component of renewable energy, plays a significant role in addressing energy and environmental challenges, thus attracting considerable attention for its conversion. Electrocatalysis and

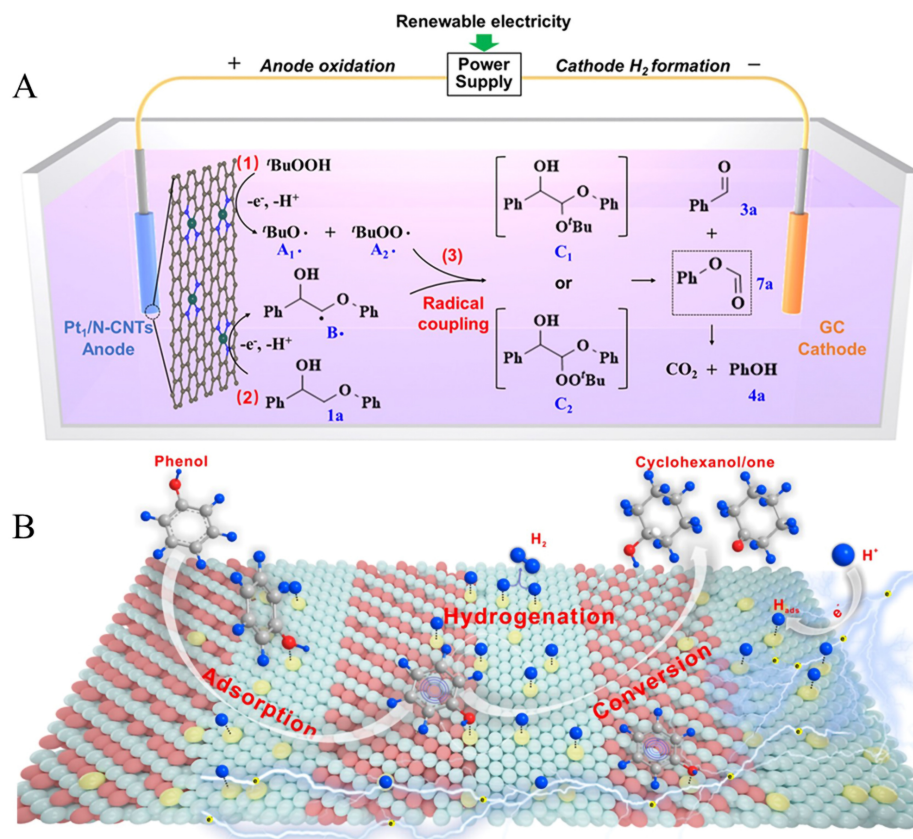


Figure 13. (A) Proposed mechanism of Pt₁/N-CNTs-catalyzed conversion of 2-phenoxy-1-phenylethanol Copyright 2021, ACS^[103]. (B) Proposed mechanism of Pt₁-CoO/Co-catalyzed hydrogenation of phenol, Copyright 2021, ACS^[104].

photoelectrocatalysis, as novel catalytic approaches, have been widely employed to achieve the conversion of various biomass-based compounds. With high catalytic activity, product selectivity, and excellent stability, SACs present broad prospects in the catalytic conversion of biomass. At present, SACs have been used in converting lignin, biomass-derived aldehydes, and alcohols, which drives the biomass valorization to high-value-added chemicals and plays an important role in promoting industrial synthesis. In biomass valorization, single-atom photoelectrocatalysts and electrocatalytic technologies demonstrate significant potential. With high-efficiency photoelectrocatalytic activity and selectivity, single-atom photoelectrocatalysts effectively promote biomass photocatalytic conversion processes such as degradation and synthesis. Simultaneously, electrocatalytic techniques leverage exceptional electrochemical activity and controllability to achieve biomass electrochemical transformations, including HMFOR and EOR, thereby reducing energy consumption in HER and facilitating the production of high-value chemicals at the anode. Single-atom catalysis within these advanced technologies offers a novel pathway for achieving sustainable biomass utilization, promising to drive future developments in sustainable energy and chemical production. However, challenges persist despite significant advancements in SACs for biomass electrocatalytic conversion. Future research directions can be categorized as follows: In SAC design, strategies such as doping, surface functionalization, nanostructuring, heteroatom substitution, and Atomic Layer Deposition (ALD) play a crucial role in modifying local environments of single-atomic sites to enhance catalytic efficiency and specificity. These methods collectively contribute to refining the local environments of single atomic sites for improved catalytic outcomes. Metal-organic frameworks (MOFs) present favorable attributes such as high surface area and adjustable pore structures, positioning them as promising choices for facilitating single atomic sites in catalysis. Carbon Nanotubes (CNTs) and Graphene, as carbon-based

materials, exhibit distinctive electronic properties and expansive surface areas, suggesting their capacity to effectively stabilize and modify the local environment of single atomic sites. LDHs showcase diverse compositions and surface functionalities, creating opportunities to tailor the surroundings of single atomic sites, potentially enhancing catalytic activity. Meanwhile, Transition Metal Carbides/Nitrides (MXenes) demonstrate high conductivity and modifiable surface chemistry, indicating their potential as support materials for single atomic sites across various catalytic applications. Particularly for larger molecules such as lignin derivatives, coupling structures of single atoms with NPs can be designed to achieve selective conversion.

Although SACs have been applied in the electrocatalytic and photo-electrocatalytic conversion of biomass-based compounds, their practicality remains limited. Future research will focus on developing multifunctional SACs capable of simultaneously catalyzing multiple biomass conversion reactions, such as hydrogenation, deoxygenation, and carbonylation, to achieve efficient, comprehensive biomass conversion. Additionally, achieving further breakthroughs based on the conversion of model compounds and directly realizing highly selective conversion of structurally complex cellulose, hemicellulose, and lignin is an important direction for future research.

DECLARATIONS

Authors' contributions

Conceptual design and project supervision: Cui T, Xu M, Hou X

Manuscript draft and revision: Ma J, Yan H, Xu M, Cui T

Availability of data and materials

Not applicable.

Financial support and sponsorship

This work was supported by the National Natural Science Foundation of China (No. 22379023, No. 22102007) and the China Postdoctoral Science Foundation (No. 2023M740555).

Conflicts of interest

All authors declared that there are no conflicts of interest.

Ethical approval and consent to participate

Not applicable.

Consent for publication

Not applicable.

Copyright

© The Author(s) 2025.

REFERENCES

1. Nanda, S.; Mohanty, P.; Pant, K. K.; Naik, S.; Kozinski, J. A.; Dalai, A. K. Characterization of North American lignocellulosic biomass and biochars in terms of their candidacy for alternate renewable fuels. *Bioenerg. Res.* **2013**, *6*, 663-77. [DOI](#)
2. Taarning, E.; Osmundsen, C. M.; Yang, X.; Voss, B.; Andersen, S. I.; Christensen, C. H. Zeolite-catalyzed biomass conversion to fuels and chemicals. *Energy. Environ. Sci.* **2011**, *4*, 793-804. [DOI](#)
3. Kavitha, S.; Yakesh, K. R.; Kasthuri, S.; et al. Profitable biomethane production from delignified rice straw biomass: the effect of lignin, energy and economic analysis. *Green. Chem.* **2020**, *22*, 8024-35. [DOI](#)
4. Deng, W.; Feng, Y.; Fu, J.; et al. Catalytic conversion of lignocellulosic biomass into chemicals and fuels. *Green. Energy. Environ.*

- 2023, 8, 10-114. DOI
5. Madadi, M.; Elsayed, M.; Sun, F.; et al. Sustainable lignocellulose fractionation by integrating p-toluenesulfonic acid/pentanol pretreatment with mannitol for efficient production of glucose, native-like lignin, and furfural. *Bioresour. Technol.* **2023**, *371*, 128591. DOI
 6. Li, X.; Xu, R.; Yang, J.; et al. Production of 5-hydroxymethylfurfural and levulinic acid from lignocellulosic biomass and catalytic upgradation. *Ind. Crop. Prod.* **2019**, *130*, 184-97. DOI
 7. Wang, T.; Nolte, M. W.; Shanks, B. H. Catalytic dehydration of C₆ carbohydrates for the production of hydroxymethylfurfural (HMF) as a versatile platform chemical. *Green. Chem.* **2014**, *16*, 548-72. DOI
 8. Gürbüz, E. I.; Gallo, J. M.; Alonso, D. M.; Wettstein, S. G.; Lim, W. Y.; Dumesic, J. A. Conversion of hemicellulose into furfural using solid acid catalysts in γ -valerolactone. *Angew. Chem. Int. Ed.* **2013**, *52*, 1270-4. DOI PubMed
 9. Devi, A.; Bajar, S.; Kour, H.; Kothari, R.; Pant, D.; Singh, A. Lignocellulosic biomass valorization for bioethanol production: a circular bioeconomy approach. *Bioenergy. Res.* **2022**, *15*, 1820-41. DOI PubMed PMC
 10. Wang, M.; Liu, M.; Lu, J.; Wang, F. Photo splitting of bio-polyols and sugars to methanol and syngas. *Nat. Commun.* **2020**, *11*, 1083. DOI PubMed PMC
 11. Yoo, C. G.; Meng, X.; Pu, Y.; Ragauskas, A. J. The critical role of lignin in lignocellulosic biomass conversion and recent pretreatment strategies: a comprehensive review. *Bioresour. Technol.* **2020**, *301*, 122784. DOI PubMed
 12. Garedeew, M.; Young-farhat, D.; Jackson, J. E.; Saffron, C. M. Electrocatalytic upgrading of phenolic compounds observed after lignin pyrolysis. *ACS. Sustain. Chem. Eng.* **2019**, *7*, 8375-86. DOI
 13. Meng, Q.; Hou, M.; Liu, H.; Song, J.; Han, B. Synthesis of ketones from biomass-derived feedstock. *Nat. Commun.* **2017**, *8*, 14190. DOI PubMed PMC
 14. Zhou, H.; Li, Z.; Xu, S. M.; et al. Selectively upgrading lignin derivatives to carboxylates through electrochemical oxidative C(OH)-C bond cleavage by a Mn-doped cobalt oxyhydroxide catalyst. *Angew. Chem. Int. Ed.* **2021**, *60*, 8976-82. DOI
 15. Kumar, R.; Strezov, V. Thermochemical production of bio-oil: a review of downstream processing technologies for bio-oil upgrading, production of hydrogen and high value-added products. *Renew. Sustain. Energy. Rev.* **2021**, *135*, 110152. DOI
 16. Pang, S. Advances in thermochemical conversion of woody biomass to energy, fuels and chemicals. *Biotechnol. Adv.* **2019**, *37*, 589-97. DOI PubMed
 17. Liu, W.; Cui, Y.; Du, X.; Zhang, Z.; Chao, Z.; Deng, Y. High efficiency hydrogen evolution from native biomass electrolysis. *Energy. Environ. Sci.* **2016**, *9*, 467-72. DOI
 18. Du, X.; Liu, W.; Zhang, Z.; et al. Low-energy catalytic electrolysis for simultaneous hydrogen evolution and lignin depolymerization. *ChemSusChem* **2017**, *10*, 847-54. DOI
 19. Tang, W.; Zhang, L.; Qiu, T.; et al. Efficient conversion of biomass to formic acid coupled with low energy consumption hydrogen production from water electrolysis. *Angew. Chem. Int. Ed.* **2023**, *62*, e202305843. DOI
 20. Zhang, X.; Wilson, K.; Lee, A. F. Heterogeneously catalyzed hydrothermal processing of C₅-C₆ sugars. *Chem. Rev.* **2016**, *116*, 12328-68. DOI
 21. Zhang, B.; Yang, Z.; Yan, C.; Xue, Z.; Mu, T. Operando forming of lattice vacancy defect in ultrathin crumpled niw-layered metal hydroxides nanosheets for valorization of biomass. *Small* **2023**, *19*, e2207236. DOI
 22. Li, S.; Wang, S.; Wang, Y.; et al. Doped Mn enhanced NiS electrooxidation performance of HMF into FDCA at industrial-level current density. *Adv. Funct. Mater.* **2023**, *33*, 2214488. DOI
 23. Cao, Y.; Zhang, H.; Ji, S.; et al. Adsorption site regulation to guide atomic design of ni-ga catalysts for acetylene semi-hydrogenation. *Angew. Chem. Int. Ed.* **2020**, *59*, 11647-52. DOI
 24. Rao, P.; Deng, Y.; Fan, W.; et al. Movable type printing method to synthesize high-entropy single-atom catalysts. *Nat. Commun.* **2022**, *13*, 5071. DOI PubMed PMC
 25. Zhao, H.; Zhu, L.; Yin, J.; et al. Stabilizing lattice oxygen through Mn doping in NiCo₂O_{4- δ} spinel electrocatalysts for efficient and durable acid oxygen evolution. *Angew. Chem. Int. Ed.* **2024**, *63*, e202402171. DOI
 26. Ye, Y.; Xu, J.; Li, X.; et al. Orbital occupancy modulation to optimize intermediate absorption for efficient electrocatalysts in water electrolysis and zinc-ethanol-air battery. *Adv. Mater.* **2024**, *36*, e2312618. DOI
 27. Wang, D.; Li, Q.; Han, C.; Lu, Q.; Xing, Z.; Yang, X. Atomic and electronic modulation of self-supported nickel-vanadium layered double hydroxide to accelerate water splitting kinetics. *Nat. Commun.* **2019**, *10*, 3899. DOI PubMed PMC
 28. Liu, S.; Gao, M.; Wu, S.; et al. A coupled electrocatalytic system with reduced energy input for CO₂ reduction and biomass valorization. *Energy. Environ. Sci.* **2023**, *16*, 5305-14. DOI
 29. Wu, X.; Zhao, Z.; Shi, X.; et al. Multi-site catalysis of high-entropy hydroxides for sustainable electrooxidation of glucose to glucaric acid. *Energy. Environ. Sci.* **2024**, *17*, 3042-51. DOI
 30. Wu, Y.; Ma, L.; Wu, J.; Song, M.; Wang, C.; Lu, J. High-surface area mesoporous Sc₂O₃ with abundant oxygen vacancies as new and advanced electrocatalyst for electrochemical biomass valorization. *Adv. Mater.* **2024**, *36*, e2311698. DOI
 31. Zheng, X.; Yang, J.; Li, P.; et al. Ir-Sn pair-site triggers key oxygen radical intermediate for efficient acidic water oxidation. *Sci. Adv.* **2023**, *9*, eadi8025. DOI PubMed PMC
 32. Yang, J.; Yang, Z.; Li, J.; et al. Engineering a hollow bowl-like porous carbon-confined Ru-MgO hetero-structured nanopair as a high-performance catalyst for ammonia borane hydrolysis. *Mater. Horiz.* **2024**, *11*, 2032-40. DOI
 33. Liu, W. J.; Xu, Z.; Zhao, D.; et al. Efficient electrochemical production of glucaric acid and H₂ via glucose electrolysis. *Nat.*

- Commun.* **2020**, *11*, 265. DOI PubMed PMC
34. Liu, C.; Shi, X. R.; Yue, K.; et al. S-species-evoked high-valence Ni^{2+δ} of the evolved β-Ni(OH)₂ electrode for selective oxidation of 5-hydroxymethylfurfural. *Adv. Mater.* **2023**, *35*, e2211177. DOI
 35. Zhou, P.; Zhang, Q.; Chao, Y.; et al. Partially reduced Pd single atoms on CdS nanorods enable photocatalytic reforming of ethanol into high value-added multicarbon compound. *Chem* **2021**, *7*, 1033-49. DOI
 36. Zhou, P.; Chao, Y.; Lv, F.; et al. Metal single atom strategy greatly boosts photocatalytic methyl activation and C-C coupling for the coproduction of high-value-added multicarbon compounds and hydrogen. *ACS. Catal.* **2020**, *10*, 9109-14. DOI
 37. Yang, W.; Jia, Z.; Zhou, B.; et al. Why is C-C coupling in CO₂ reduction still difficult on dual-atom electrocatalysts? *ACS. Catal.* **2023**, *13*, 9695-705. DOI
 38. Zhang, Z.; Wang, J.; Ge, X.; et al. Mixed plastics wastes upcycling with high-stability single-atom Ru catalyst. *J. Am. Chem. Soc.* **2023**, *145*, 22836-44. DOI
 39. Liu, J.; Lucci, F. R.; Yang, M.; et al. Tackling CO poisoning with single-atom alloy catalysts. *J. Am. Chem. Soc.* **2016**, *138*, 6396-9. DOI
 40. Xia, J.; Wang, B.; Di, J.; et al. Construction of single-atom catalysts for electro-, photo- and photoelectro-catalytic applications: State-of-the-art, opportunities, and challenges. *Mater. Today.* **2022**, *53*, 217-37. DOI
 41. Nakaya, Y.; Hirayama, J.; Yamazoe, S.; Shimizu, K. I.; Furukawa, S. Single-atom Pt in intermetallics as an ultrastable and selective catalyst for propane dehydrogenation. *Nat. Commun.* **2020**, *11*, 2838. DOI PubMed PMC
 42. Cao, L.; Luo, Q.; Liu, W.; et al. Identification of single-atom active sites in carbon-based cobalt catalysts during electrocatalytic hydrogen evolution. *Nat. Catal.* **2019**, *2*, 134-41. DOI
 43. Vasconcelos, S. C.; Marchini, L.; Lima, C. G. S.; et al. Single-atom catalysts for the upgrading of biomass-derived molecules: an overview of their preparation, properties and applications. *Green. Chem.* **2022**, *24*, 2722-51. DOI
 44. Gan, T.; Wang, D. Atomically dispersed materials: Ideal catalysts in atomic era. *Nano. Res.* **2024**, *17*, 18-38. DOI
 45. Cui, T.; Li, L.; Ye, C.; et al. Heterogeneous single atom environmental catalysis: fundamentals, applications, and opportunities. *Adv. Funct. Mater.* **2022**, *32*, 2108381. DOI
 46. Wang, L.; Wang, L.; Zhang, L.; Liu, H.; Yang, J. Perspective of p-block single-atom catalysts for electrocatalysis. *Trends. Chem.* **2022**, *4*, 1135-48. DOI
 47. Qi, H.; Yang, J.; Liu, F.; et al. Highly selective and robust single-atom catalyst Ru₁/NC for reductive amination of aldehydes/ketones. *Nat. Commun.* **2021**, *12*, 3295. DOI PubMed PMC
 48. Liu, Z.; Li, H.; Gao, X.; et al. Rational highly dispersed ruthenium for reductive catalytic fractionation of lignocellulose. *Nat. Commun.* **2022**, *13*, 4716. DOI PubMed PMC
 49. Li, S.; Dong, M.; Yang, J.; et al. Selective hydrogenation of 5-(hydroxymethyl)furfural to 5-methylfurfural over single atomic metals anchored on Nb₂O₅. *Nat. Commun.* **2021**, *12*, 584. DOI PubMed PMC
 50. Liu, Y.; Gan, T.; He, Q.; Zhang, H.; He, X.; Ji, H. Catalytic oxidation of 5-hydroxymethylfurfural to 2,5-diformylfuran over atomically dispersed ruthenium catalysts. *Ind. Eng. Chem. Res.* **2020**, *59*, 4333-7. DOI
 51. Liu, S.; Bai, L.; van, M. A. P.; et al. Oxidative cleavage of β-O-4 bonds in lignin model compounds with a single-atom Co catalyst. *Green. Chem.* **2019**, *21*, 1974-81. DOI
 52. Meng, G.; Ji, K.; Zhang, W.; et al. Tandem catalyzing the hydrodeoxygenation of 5-hydroxymethylfurfural over a Ni₃Fe intermetallic supported Pt single-atom site catalyst. *Chem. Sci.* **2021**, *12*, 4139-46. DOI PubMed PMC
 53. Lou, Y.; Zhao, Y.; Liu, H.; et al. Edge-confined Pt₁/MoS₂ single-atom catalyst promoting the selective activation of carbon-oxygen bond. *ChemCatChem* **2021**, *13*, 2783-93. DOI
 54. Zhu, M.; Du, X.; Zhao, Y.; et al. Ring-opening transformation of 5-hydroxymethylfurfural using a golden single-atomic-site palladium catalyst. *ACS. Catal.* **2019**, *9*, 6212-22. DOI
 55. Li, Z.; Dong, X.; Zhang, M.; et al. Selective hydrogenation on a highly active single-atom catalyst of palladium dispersed on ceria nanorods by defect engineering. *ACS. Appl. Mater. Interfaces.* **2020**, *12*, 57569-77. DOI
 56. Meng, W.; Sun, S.; Xie, D.; et al. Engineering defective Co₃O₄ containing both metal doping and vacancy in octahedral cobalt site as high performance catalyst for methane oxidation. *Mol. Catal.* **2024**, *553*, 113768. DOI
 57. De, S.; Burange, A. S.; Luque, R. Conversion of biomass-derived feedstocks into value-added chemicals over single-atom catalysts. *Green. Chem.* **2022**, *24*, 2267-86. DOI
 58. Chen, J.; Xiao, Y.; Guo, F.; Li, K.; Huang, Y.; Lu, Q. Single-atom metal catalysts for catalytic chemical conversion of biomass to chemicals and fuels. *ACS. Catal.* **2024**, *14*, 5198-226. DOI
 59. Wang, D.; Shan, H.; Yin, W.; Li, H. Defect engineering of single-atom catalysts in biomass conversion. *Fuel* **2024**, *355*, 129439. DOI
 60. Lu, Y.; Zhang, Z.; Wang, H.; Wang, Y. Toward efficient single-atom catalysts for renewable fuels and chemicals production from biomass and CO₂. *Appl. Catal. B. Environ.* **2021**, *292*, 120162. DOI
 61. Zhuang, J.; Wang, D. Recent advances of single-atom alloy catalyst: properties, synthetic methods and electrocatalytic applications. *Mater. Today. Catal.* **2023**, *2*, 100009. DOI
 62. Lu, Y.; Liu, T.; Dong, C. L.; et al. Tuning the selective adsorption site of biomass on Co₃O₄ by Ir single atoms for electrosynthesis. *Adv. Mater.* **2021**, *33*, e2007056. DOI
 63. Ge, R.; Wang, Y.; Li, Z.; et al. Selective electrooxidation of biomass-derived alcohols to aldehydes in a neutral medium: promoted

- water dissociation over a nickel-oxide-supported ruthenium single-atom catalyst. *Angew. Chem. Int. Ed.* **2022**, *61*, e202200211. DOI
64. Gu, W.; Pei, A.; Zhang, S.; et al. Atomic-interface effect of single-atom Ru/CoO_x for selective electrooxidation of 5-hydroxymethylfurfural. *ACS Appl. Mater. Interfaces.* **2023**, *15*, 28036-43. DOI
65. Xu, H.; Xin, G.; Hu, W.; et al. Single-atoms Ru/NiFe layered double hydroxide electrocatalyst: efficient for oxidation of selective oxidation of 5-hydroxymethylfurfural and oxygen evolution reaction. *Appl. Catal. B. Environ.* **2023**, *339*, 123157. DOI
66. Zeng, L.; Chen, Y.; Sun, M.; et al. Cooperative Rh-O₂/Ni(Fe) site for efficient biomass upgrading coupled with H₂ production. *J. Am. Chem. Soc.* **2023**, *145*, 17577-87. DOI
67. Ji, K.; Xu, M.; Xu, S. M.; et al. Electrocatalytic hydrogenation of 5-hydroxymethylfurfural promoted by a Ru₁ Cu single-atom alloy catalyst. *Angew. Chem. Int. Ed.* **2022**, *61*, e202209849. DOI
68. Zhou, Y.; Slater, T. J.; Luo, X.; Shen, Y. A versatile single-copper-atom electrocatalyst for biomass valorization. *Appl. Catal. B. Environ.* **2023**, *324*, 122218. DOI
69. Wu, Y.; Jiang, Y.; Chen, W.; et al. Selective electroreduction of 5-hydroxymethylfurfural to dimethylfuran in neutral electrolytes via hydrogen spillover and adsorption configuration adjustment. *Adv. Mater.* **2024**, *36*, e2307799. DOI
70. Zhou, P.; Chen, Y.; Luan, P.; et al. Selective electrochemical hydrogenation of furfural to 2-methylfuran over a single atom Cu catalyst under mild pH conditions. *Green. Chem.* **2021**, *23*, 3028-38. DOI
71. Mukadam, Z.; Liu, S.; Pedersen, A.; et al. Furfural electrovalorisation using single-atom molecular catalysts. *Energy. Environ. Sci.* **2023**, *16*, 2934-44. DOI
72. Wang, Y.; Zhu, Y.; Xie, Z.; et al. Efficient electrocatalytic oxidation of glycerol via promoted OH* generation over single-atom-bismuth-doped spinel Co₃O₄. *ACS. Catal.* **2022**, *12*, 12432-43. DOI
73. Yu, H.; Wang, W.; Mao, Q.; et al. Pt single atom captured by oxygen vacancy-rich NiCo layered double hydroxides for coupling hydrogen evolution with selective oxidation of glycerol to formate. *Appl. Catal. B. Environ.* **2023**, *330*, 122617. DOI
74. Feng, X.; Sun, T.; Feng, X.; et al. Single-atomic-site platinum steers middle hydroxyl selective oxidation on amorphous/crystalline homojunction for photoelectrochemical glycerol oxidation coupled with hydrogen generation. *Adv. Funct. Mater.* **2024**, *34*, 2316238. DOI
75. Tian, Z.; Da, Y.; Wang, M.; et al. Selective photoelectrochemical oxidation of glucose to glucaric acid by single atom Pt decorated defective TiO₂. *Nat. Commun.* **2023**, *14*, 142. DOI PubMed PMC
76. Ayele, A. A.; Tsai, M.; Adam, D. B.; et al. Electrochemical oxidation of ethylene glycol on TiO₂-supported platinum single-atom catalyst into valuable chemicals in alkaline media. *Appl. Catal. A. Gen.* **2022**, *646*, 118861. DOI
77. Moges, E. A.; Chang, C.; Huang, W.; et al. Sustainable synthesis of dual single-atom catalyst of Pd-N₄/Cu-N₄ for partial oxidation of ethylene glycol. *Adv. Funct. Mater.* **2022**, *32*, 2206887. DOI
78. Chen, W.; Luo, X.; Slater, T. J. A.; et al. General synthesis of single atom electrocatalysts via a facile condensation-carbonization process. *J. Mater. Chem. A.* **2020**, *8*, 25959-69. DOI
79. Ayele, A. A.; Tsai, M.; Awoke, Y. A.; et al. Ni-doped TiO₂ supported Pt single-atom catalyst for partial oxidation of ethylene glycol to high-value chemicals in alkaline media. *Mater. Today. Chem.* **2023**, *34*, 101797. DOI
80. Liu, R.; Zhang, L. Q.; Yu, C.; Sun, M. T.; Liu, J. F.; Jiang, G. B. Atomic-level-designed catalytically active palladium atoms on ultrathin gold nanowires. *Adv. Mater.* **2017**, *29*, 1604571. DOI PubMed
81. Tiwari, J. N.; Dang, N. K.; Park, H. J.; et al. Remarkably enhanced catalytic activity by the synergistic effect of palladium single atoms and palladium-cobalt phosphide nanoparticles. *Nano. Energy.* **2020**, *78*, 105166. DOI
82. Li, M.; Duanmu, K.; Wan, C.; et al. Single-atom tailoring of platinum nanocatalysts for high-performance multifunctional electrocatalysis. *Nat. Catal.* **2019**, *2*, 495-503. DOI
83. Li, S.; Guan, A.; Wang, H.; et al. Hybrid palladium nanoparticles and nickel single atom catalysts for efficient electrocatalytic ethanol oxidation. *J. Mater. Chem. A.* **2022**, *10*, 6129-33. DOI
84. Zhang, B.; Lai, W.; Sheng, T.; et al. Ordered platinum-bismuth intermetallic clusters with Pt-skin for a highly efficient electrochemical ethanol oxidation reaction. *J. Mater. Chem. A.* **2019**, *7*, 5214-20. DOI
85. Luo, S.; Zhang, L.; Liao, Y.; et al. A tensile-strained Pt-Rh single-atom alloy remarkably boosts ethanol oxidation. *Adv. Mater.* **2021**, *33*, e2008508. DOI
86. Zhang, G.; Cao, D.; Guo, S.; et al. Tuning the selective ethanol oxidation on tensile-trained Pt(110) surface by Ir single atoms. *Small* **2022**, *18*, e2202587. DOI
87. Zhang, G.; Hui, C.; Yang, Z.; et al. Hydrogen-induced p-d orbital hybridization and tensile strain of PdGa single-atom alloy metallene boosts complete electrooxidation of ethanol. *Appl. Catal. B. Environ.* **2024**, *342*, 123377. DOI
88. Lan, B.; Huang, M.; Wei, R. L.; Wang, C. N.; Wang, Q. L.; Yang, Y. Y. Ethanol electrooxidation on rhodium-lead catalysts in alkaline media: high mass activity, long-term durability, and considerable CO₂ selectivity. *Small* **2020**, *16*, e2004380. DOI
89. Zhu, C.; Lan, B.; Wei, R.; Wang, C.; Yang, Y. Potential-dependent selectivity of ethanol complete oxidation on rh electrode in alkaline media: a synergistic study of electrochemical ATR-SEIRAS and IRAS. *ACS. Catal.* **2019**, *9*, 4046-53. DOI
90. Chang, Q.; Hong, Y.; Lee, H. J.; et al. Achieving complete electrooxidation of ethanol by single atomic Rh decoration of Pt nanocubes. *Proc. Natl. Acad. Sci. USA.* **2022**, *119*, e2112109119. DOI PubMed PMC
91. Pei, A.; Li, G.; Zhu, L.; et al. Nickel hydroxide-supported Ru single atoms and Pd nanoclusters for enhanced electrocatalytic hydrogen evolution and ethanol oxidation. *Adv. Funct. Mater.* **2022**, *32*, 2208587. DOI
92. Wang, H.; Jiao, L.; Zheng, L.; et al. PdBi single-atom alloy aerogels for efficient ethanol oxidation. *Adv. Funct. Mater.* **2021**, *31*,

2103465. DOI
93. Zhang, Z.; Liu, J.; Wang, J.; et al. Single-atom catalyst for high-performance methanol oxidation. *Nat. Commun.* **2021**, *12*, 5235. DOI PubMed PMC
 94. Poerwoprajitno, A. R.; Gloag, L.; Watt, J.; et al. A single-Pt-atom-on-Ru-nanoparticle electrocatalyst for CO-resilient methanol oxidation. *Nat. Catal.* **2022**, *5*, 231-7. DOI
 95. Chen, L.; Liang, X.; Wang, D.; et al. Platinum-ruthenium single atom alloy as a bifunctional electrocatalyst toward methanol and hydrogen oxidation reactions. *ACS Appl. Mater. Interfaces.* **2022**, *14*, 27814-22. DOI
 96. Kong, F.; Liu, X.; Song, Y.; et al. Selectively coupling Ru single atoms to PtNi concavities for high-performance methanol oxidation via d-band center regulation. *Angew. Chem. Int. Ed.* **2022**, *61*, e202207524. DOI
 97. Zhuang, L.; Jia, Z.; Wang, Y.; et al. Nitrogen-doped carbon black supported synergistic palladium single atoms and nanoparticles for electrocatalytic oxidation of methanol. *Chem. Eng. J.* **2022**, *438*, 135585. DOI
 98. Ruan, J.; Chen, Y.; Zhao, G.; et al. Cobalt single atoms enabling efficient methanol oxidation reaction on platinum anchored on nitrogen-doped carbon. *Small* **2022**, *18*, e2107067. DOI
 99. Lv, J.; Feng, W.; Yang, S.; Liu, H.; Huang, X. Methanol dissociation and oxidation on single Fe atom supported on graphitic carbon nitride. *Appl. Organom. Chem.* **2019**, *33*, e4930. DOI
 100. Fan, X.; Chen, W.; Xie, L.; et al. Surface-enriched single-Bi-atoms tailoring of Pt nanorings for direct methanol fuel cells with ultralow-Pt-loading. *Adv. Mater.* **2024**, *36*, e2313179. DOI
 101. Wei, X.; Zhang, J.; Liu, C.; Han, X.; Deng, Y.; Hu, W. Ir single atoms doped cubooctahedral Pd for boosted methanol oxidation reaction. *Part. Part. Syst. Charact.* **2022**, *39*, 2200013. DOI
 102. Miao, J.; Ma, Y.; Wang, X.; et al. Efficiently selective C(O-)-C bond cleavage for full lignocellulose upgrading coupled with energy-saving hydrogen production by Ir single-atom electrocatalyst. *Appl. Catal. B. Environ.* **2023**, *336*, 122937. DOI
 103. Cui, T.; Ma, L.; Wang, S.; et al. Atomically Dispersed Pt-N₃C₁ sites enabling efficient and selective electrocatalytic C-C bond cleavage in lignin models under ambient conditions. *J. Am. Chem. Soc.* **2021**, *143*, 9429-39. DOI
 104. Tong, S.; Gao, X.; Zhou, H.; Shi, Q.; Wu, Y.; Chen, W. Synergistic roles of the CoO/Co heterostructure and Pt single atoms for high-efficiency electrocatalytic hydrogenation of lignin-derived Bio-Oils. *Inorg. Chem.* **2023**, *62*, 19123-34. DOI